Volume 4, Issue 7— January — June - 2020

ECORFAN

# Journal- Taiwan

ISSN-On line 2524-2121

ECORFAN®

**ECORFAN Journal-Taiwan**, Volume 4, Issue 7, January - June 2020, is a journal edited semestral by ECORFAN. Taiwan, Taipei. YongHe district, Zhong Xin, Street 69. Postcode: 23445. WEB: www.ecorfan.org/taiwan/journal@ecorfan.org. Editor in Chief: VARGAS-DELGADO, Oscar. PhD. ISSN: 2524-2121. Responsible for the latest update of this number ECORFAN Computer Unit. ESCAMILLA-BOUCHÁN, Imelda. PhD, LUNA-SOTO, Vladimir. PhD, last updated June 30, 2020.

# ECORFAN Journal- Taiwan

## Definition of Journal

## Scientific Objectives

Support the international scientific community in its written production Science, Technology and Innovation in the Field of Physical Sciences Mathematics and Earth sciences, in Subdisciplines of optical astronomy, optical characterization, optical encoder, experimental research, planetary magnetic fields, ultraviolet radiation, lasers, algorithms and optical waves.

ECORFAN-Mexico SC is a Scientific and Technological Company in contribution to the Human Resource training focused on the continuity in the critical analysis of International Research and is attached to CONACYT-RENIECYT number 1702902, its commitment is to disseminate research and contributions of the International Scientific Community, academic institutions, agencies and entities of the public and private sectors and contribute to the linking of researchers who carry out scientific activities, technological developments and training of specialized human resources with governments, companies and social organizations.

Encourage the interlocution of the International Scientific Community with other Study Centers in Mexico and abroad and promote a wide incorporation of academics, specialists and researchers to the publication in Science Structures of Autonomous Universities - State Public Universities - Federal IES - Polytechnic Universities - Technological Universities - Federal Technological Institutes - Normal Schools - Decentralized Technological Institutes - Intercultural Universities - S & T Councils - CONACYT Research Centers.

## Scope, Coverage and Audience

ECORFAN Journal- Taiwan is a Journal edited by ECORFAN-Mexico S.C in its Holding with repository in Taiwan, is a scientific publication arbitrated and indexed with semester periods. It supports a wide range of contents that are evaluated by academic peers by the Double-Blind method, around subjects related to the theory and practice of optical astronomy, optical characterization, optical encoder, experimental research, planetary magnetic fields, ultraviolet radiation, lasers, algorithms and optical waves with diverse approaches and perspectives , That contribute to the diffusion of the development of Science Technology and Innovation that allow the arguments related to the decision making and influence in the formulation of international policies in the Field of Physical Sciences Mathematics and Earth sciences. The editorial horizon of ECORFAN-Mexico® extends beyond the academy and integrates other segments of research and analysis outside the scope, as long as they meet the requirements of rigorous argumentative and scientific, as well as addressing issues of general and current interest of the International Scientific Society.

**Arbitration Committee**

**Assignment of Rights**

The sending of an Article to ECORFAN Journal- Taiwan emanates the commitment of the author not to submit it simultaneously to the consideration of other series publications for it must complement the Originality Format for its Article.

The authors sign the Authorization Format for their Article to be disseminated by means that ECORFAN-Mexico, S.C. In its Holding Taiwan considers pertinent for disclosure and diffusion of its Article its Rights of Work.

**Declaration of Authorship**

Indicate the Name of Author and Coauthors at most in the participation of the Article and indicate in extensive the Institutional Affiliation indicating the Department.

Identify the Name of Author and Coauthors at most with the CVU Scholarship Number-PNPC or SNI-CONACYT- Indicating the Researcher Level and their Google Scholar Profile to verify their Citation Level and H index.

Identify the Name of Author and Coauthors at most in the Science and Technology Profiles widely accepted by the International Scientific Community ORC ID - Researcher ID Thomson - arXiv Author ID - PubMed Author ID - Open ID respectively.

Indicate the contact for correspondence to the Author (Mail and Telephone) and indicate the Researcher who contributes as the first Author of the Article.

**Plagiarism Detection**

All Articles will be tested by plagiarism software PLAGSCAN if a plagiarism level is detected Positive will not be sent to arbitration and will be rescinded of the reception of the Article notifying the Authors responsible, claiming that academic plagiarism is criminalized in the Penal Code.

**Arbitration Process**

All Articles will be evaluated by academic peers by the Double Blind method, the Arbitration Approval is a requirement for the Editorial Board to make a final decision that will be final in all cases. MARVID® is a derivative brand of ECORFAN® specialized in providing the expert evaluators all of them with Doctorate degree and distinction of International Researchers in the respective Councils of Science and Technology the counterpart of CONACYT for the chapters of America-Europe-Asia- Africa and Oceania. The identification of the authorship should only appear on a first removable page, in order to ensure that the Arbitration process is anonymous and covers the following stages: Identification of the Journal with its author occupation rate - Identification of Authors and Coauthors - Detection of plagiarism PLAGSCAN - Review of Formats of Authorization and Originality-Allocation to the Editorial Board-Allocation of the pair of Expert Arbitrators-Notification of Arbitration -Declaration of observations to the Author-Verification of Article Modified for Editing-Publication.

**Instructions for Scientific, Technological and Innovation Publication**

**Knowledge Area**

The works must be unpublished and refer to topics of optical astronomy, optical characterization, optical encoder, experimental research, planetary magnetic fields, ultraviolet radiation, lasers, algorithms and optical waves and other topics related to Physical Sciences Mathematics and Earth sciences.

## Presentation of the content

In the first article we present, *Solar Concentrator PDR with solar tracking*, by DURAN, Pino, BARBOSA, J. Gabriel, QUINTO, Pedro and MORENO, Luis, in the next article we present, *Mechatronic system to assist rehabilitation therapies for shoulder and elbow joints: Design, kinematic analysis, building and HMI*, by AGUILAR-PEREYRA, Felipe, ALVARADO, Jorge, ALEGRIA, Jesús and SOSA, José, with adscription in the Universidad Tecnológica de Querétaro, in the next article we present, *Image resolution enhancement via sparse interpolation on wavelet domain*, by CHAVEZ, Román, PONOMARYOW, Volodymyr and CASTRO, Fernando, with adscription in the Universidad Tecnológica de la Región Norte de Guerrero, in the last article we present, *Prototype robot rover with Arduino, LabVIEW and mobile devices*, by BELTRAN, Miguel, SALINAS, Oscar and LUNA-ORTIZ, Martha, with adscription in the Universidad Tecnológica Emiliano Zapata del Estado de Morelos.

## Content

**Article** **ECORFAN Journal- Taiwan**
June, 2020 Vol.4 No.7 1-8

# Solar Concentrator PDR with solar tracking

# Concentrador Solar PDR con seguimiento solar

DURAN, Pino†*, BARBOSA, J. Gabriel, QUINTO, Pedro and MORENO, Luis

ID 1st Author: *Pino, Duran*

ID 1st Coauthor: *J. Gabriel, Barbosa*

ID 2nd Coauthor: *Pedro, Quinto*

ID 3rd Coauthor: *Luis, Moreno*

**DOI:** 10.35429/EJT.2020.7.4.1.8 Received March 02, 2020; Accepted June 30, 2020

**Abstract**

The reduction in conventional fuels consumption can be accomplished through the use of solar energy, transforming it into thermal energy throught a solar collector. There are a lot of solar collector kind, but the solar concentration way, specifically the parabolic dish reflector technology, or just PDR solar concentrator, offers one of the most efficient paths to achieve high quality thermal energy. Usually, the PDR solar concentrator are designed in big dimensions in order to generate electrical energy; nevertheless this technology could be used in minor scale in order to generate solar concentration high levels to achieve enough thermal energy to satisfy hot water demand in residential buildings, homes and even the industry. The prototype here presented was developed in four phases: The parabolic dish, the gear box and mechanical support device, the sun tracking control system and finally the system integration and operational tests. The four phases conjunction results in a totally operative prototype with the capability of achieve temperatures of 400 ºC, over a concentration focal point under partially cloudy day conditions.

**Prototype, Solar energy, Thermal energy, Solar concentrator, PDR, Sun tracking, Parabolic dish.**

**Resumen**

La reducción en el consumo de combustibles convencionales puede realizarse a través del uso de la energía solar, transformándola en energía térmica a través de un colector solar que de entre todos los tipos existentes, la tecnología del colector de concentración de disco parabólico reflector, o simplemente concentrador solar PDR, presenta una de las vías de mayor eficiencia para la obtención de energía térmica. Los concentradores solares de disco parabólico reflector, usualmente son diseñados en grandes dimensiones con el propósito de generar energía eléctrica, sin embargo esta misma tecnología, pero a pequeña escala, es capaz de alcanzar elevados niveles de concentración solar generando así energía térmica suficiente para satisfacer la demanda de agua caliente en edificios habitacionales, casas e incluso en la industria. El prototipo que en este trabajo se presenta fue desarrollado en cuatro fases: El disco parabólico, las cajas de engranes y dispositivo de soporte, el sistema de control para el seguimiento solar y finalmente la integración y pruebas de operación. La conjunción de las cuatro fases resulta en un prototipo totalmente operativo con la capacidad de llegar hasta los 400 °C de temperatura sobre el punto focal de concentración bajo condiciones de día parcialmente nublado.

**Prototipo, Energía solar, Energía térmica, Concentrador solar, PDR, Seguimiento solar, Disco parabólico**

**Citation:** DURAN, Pino, BARBOSA, J. Gabriel, QUINTO, Pedro and MORENO, Luis. Solar Concentrator PDR with solar tracking. ECORFAN Journal-Taiwan. 2020. 4-7: 1-8

* Author correspondence (pinoduran@hotmail.com)
† Researcher contributing as first author.

 

## Introduction

Solar energy is a viable alternative to solve the energy problems that the use of fossil fuels entails. There is a lot of information about the behavior of this energy, in what magnitude it is received on our planet and especially in Mexico. Currently, both public and private organizations worldwide are making great efforts to generate knowledge and technological advances in order to achieve a better capture of solar energy in an increasingly economical and efficient way (Perales, 2007). They have developed a series of experimental models and from them it has been tried to improve them more and more, however, these improvements carry with them an inevitable increase in manufacturing costs.

There are various technologies of solar collectors whose efficiencies depend on the capacity to capture solar radiation, the most widely used being the flat collector type, however, its concentration is relatively low compared to other technologies used at gigantic industrial levels, such is the case concentration collectors, specifically the parabolic reflector disk. Until now, concentration technology has generally been handled only on a large scale, that is, from 5 to 7 m in diameter, thus justifying the demand for electrical energy necessary to move the collector in two rotational axes, which precisely gives it the possibility of reach high levels of concentration.

The purpose of this work is to design and build a prototype of a PDR solar concentrator, or reflector disk parabolic, with solar tracking in two axes, whose diameter is of small modularity and that provides high quality thermal energy, that is, high temperature. The reason for providing a disk of small dimensions lies in making concentrating solar technology applicable both to satisfy the needs of thermal energy for services and uses of small and medium-sized industries as well as for homes, and is no longer exclusive to the production of steam for power generation.

The design and construction process, as well as integration and testing, of the small modularity PDR solar concentrator is presented in four sections: Configuration of the concentrator disk, the design criteria and the final construction of the concentrator disk are presented.

Clamping and movement mechanisms, the elements used for the transmission of movement to the concentrator are presented; Control system for solar tracking, the form of control chosen to carry out solar tracking in two axes is disclosed; Results, the experimental data obtained once all the parts of the concentrator have been integrated are presented.

## Hub Disk Configuration

The dimensions of the reflector parabolic disk are determined from the geometric relationships shown in Figure 1 in which it can be observed that there is a relationship between the diameter of the disk, a, the focal length, f, and the edge angle. , ϕr, depending on the width of the focal image, W, required so that a heat transfer device can be placed in the center of the concentrator (Kalogirou, 2009).

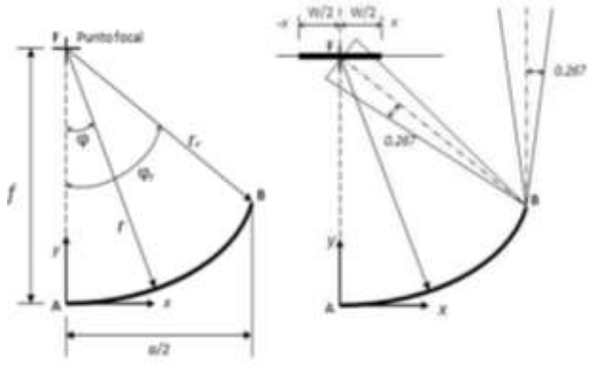


**Figure 1** Geometric parameters of a reflecting parabolic disk

When designing any type of solar collector, the main objective is to obtain the best possible use of the solar radiation captured. In the case of concentration collectors, this use depends on the concentration ratio, finding that the main design criterion to be established is the maximum concentration ratio Cmax, and this value must be kept constant to carry out the sizing of both the disk and the absorber element.

This Cmax value is defined as the maximum that can be obtained, based on the interception of all the reflected specular radiation which is within the cone with angular amplitude equal to 0.534 + δ as shown in Figure 2. According to Duffie and Beckman (2009), this maximum value mathematically is obtained as follows:

ISSN 2524-2121

$$C_{max} = \frac{sen^2\varphi_r cos^2(\varphi_r + 0.267 + \frac{\delta}{2})}{4sen^2(0.267 + \frac{\delta}{2})} - 1 \quad (1)$$

The inclusion of the factor called scattering angle, δ, makes it possible to consider the angular errors associated with inappropriate solar tracking, roughness inherent to the reflecting surface and poorly shaped in the curvature of the disk. That is, depending on these errors, it can be known how much the radiation reflected by the concentrating element increases in amplitude. These standard errors have been obtained experimentally using statistics (Stine, 1985).

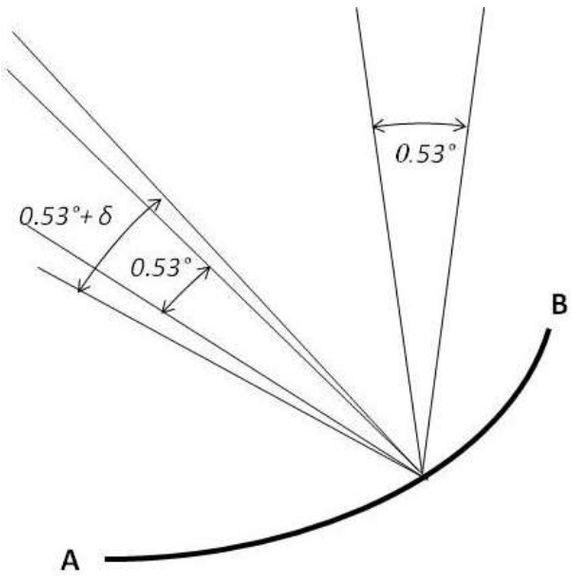


**Figure 2** Schematic of a portion of a concentrator with a scattering angle δ added to the solar interception angle of 0.53 °.

From equation 1 it can be seen that the Cmax depends on the edge angle φr, in this way various values of it will have to be proposed to know the maximum value of Cmax that could be reached.

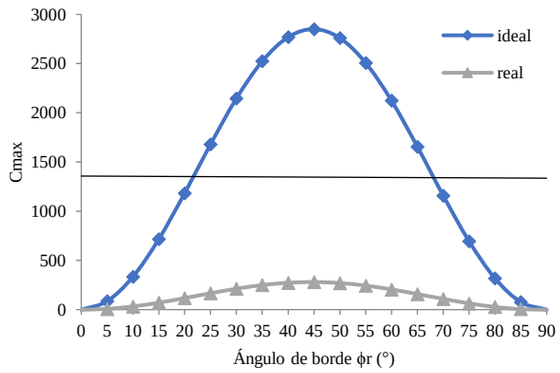


**Graphic 1** Maximum concentration ratio for PDR collectors

In Graph 1 it can be seen that the maximum value of Cmax is 2850 and is reached when °r = 45 °, after 45 ° the value of Cmax begins to decline in the same proportion as it increased. However, only the ideal case has been considered, it is possible to compare the ideal case with the behavior of Cmax by including the angular deviation. According to the graph φr against Cmax, it is observed that the maximum concentration ratio decreases drastically from 2850 to 280 when including the angular dispersion, that is, it decreases almost 10 times its value.

The values of φr = 45 ° and Cmax, real = 280 are considered as the first design criteria for the reflector parabolic disk and must be kept constant to determine the geometric parameters of the disk.

The second design criterion of the parabolic disk is the fulfillment of one of the objectives of this work, the small modularity of the concentrator, which must be small to be installed in a house but large enough to be able to couple some type heat exchanger at its focal point, for example thermosiphon type.

Having the edge angle defined to achieve the highest concentration, it is now necessary to establish the edge radius and the optimal focal length to generate an image on the focal plane such that it allows satisfying the criterion of small modularity.

According to the results obtained, disc diameters less than 1 m provide very small focal images to consider the construction of a functional heat exchanger. The diameters of 1 m, 1.25 m and 1.5 m generate focal images on which thermosyphon-type heat exchangers of at least 2.54 cm in diameter could well be constructed.

Disc diameters of 1.75 m onwards are considered too large to meet the small modularity criterion (Durán, 2012).

Therefore, the diameter of the disk proposed for the construction of the parabolic disk will be defined at a value of 1.5 m since its corresponding image width will allow a thermosyphon of almost 5 cm in diameter to be placed on its focal point, allowing a better use of the radiation solar.

Table 1 summarizes the geometric characteristics and technical specifications of the concentrator and absorber and is illustrated in Figure 3.

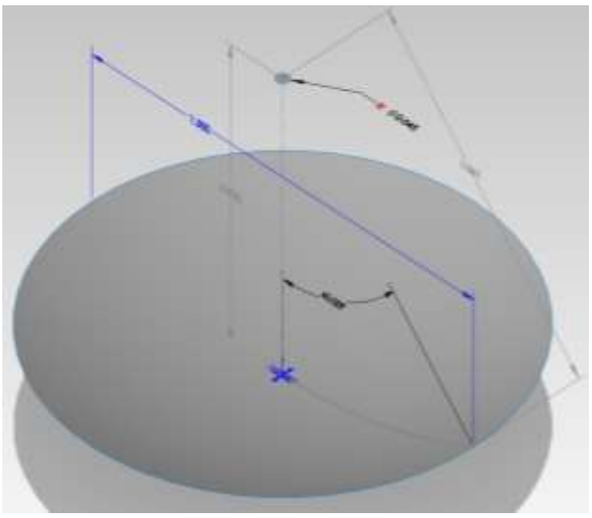

**Figure 3** Graphic design of the reflector disc and absorber element

| Characteristic | Specification |
|---|---|
| Collecting area | 12.55 $m^2$ |
| Edge angle | 45° |
| Diameter | 1.5 m |
| Focal distance | 0.9 m |
| Edge Radius | 1.06 m |
| Disc mold | Fiberglass |
| Reflective material | Mylar |
| Mylar reflectivity | 0.85 |
| Absorber diameter | 0.05 m |
| Absorber material | Aluminum |
| Anodized aluminum absorptivity | 0.14 |
| Total weight | 20 kg |

**Table 1** Technical specifications of the concentrator disc and absorber element

## Mechanisms of movement and clamping

The mechanical system of the concentrator is made up of two parts. The first is a gearbox manufactured in duplicate in order to allow the transmission of motion from the motors to each axis of rotation (two-axis tracking mechanism). The second refers to the support structure to mount the rotation shafts that in turn will support the reflector disk.

The motor considered suitable for the movement of the concentrator is an automotive worm-worm type motor, since it provides high torque at low speed and a transmission of unidirectional movement from the motor to the mass of the concentrator.

The design of a gearbox or speed reducer is of great importance for the solar concentrator, since through it it is possible to obtain the precision of the angular movement in each axis.

So that for every half turn of the axis of the worm gear, the elevation or azimuth axis has an angular displacement of 1 °. In order for the box to be neither too heavy nor robust, a 4-gear design like the one shown in Figure 4 is proposed.

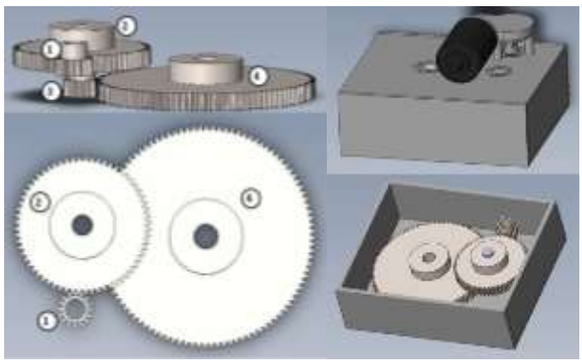

**Figure 4** Gear train for transmission of motion and speed reduction

Figure 5 shows the proposed design for the support system, which tries to concentrate all the weight of the concentrator just on the vertical axis so that there is no weight imbalance during the movement of the prototype, perhaps caused by the disc itself. reflector or gearboxes, these two components being the heaviest.

As it is a solar concentrator that must be following the Sun throughout the day, it is required that the main components of the support are in a certain way resistant to corrosive effects and deterioration due to the weather, so the material of the bars that make up the shafts are made of stainless steel.

The main mechanical components are mentioned in Table 2 and are indicated in Figure 5, which corresponds to the design of the PDR solar concentrator.

ISSN 2524-2121

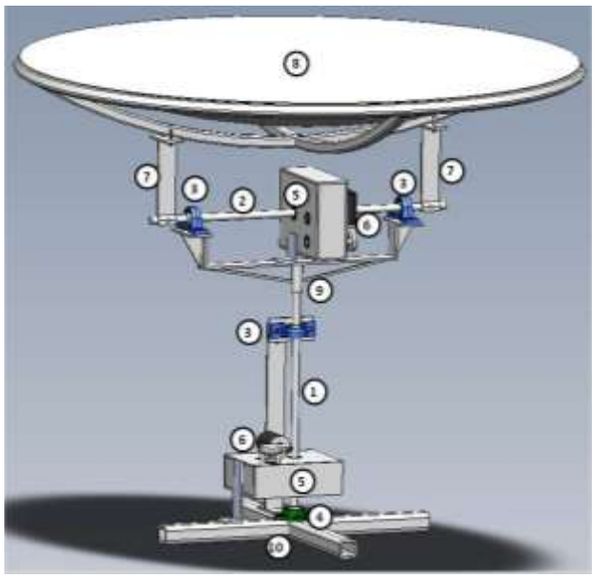

**Figure 5** PDR Solar Concentrator General Design

| No. | Component / Part |
|---|---|
| 1 | Vertical axis of rotation for azimuth. |
| 2 | Horizontal axis of rotation for lifting |
| 3 | Bearings for the two axes, vertical and horizontal. |
| 4 | Bearing for vertical axis. |
| 5 | Gear box. |
| 6 | Engine. |
| 7 | Disc support arms. |
| 8 | Reflector disk. |
| 9 | Vertical axis support. |
| 10 | Base. |

**Table 2** Components and main mechanical parts of the concentrator

## Control system for solar tracking

When working with concentrating solar collectors, it is necessary to develop a solar tracking system in one or two axes depending on the type of collector, since they work mainly with direct solar radiation. In the case of parabolic disk concentrators, a solar tracking is managed in two axes, elevation and azimuth, with the aim that the concentrator is always oriented to the Sun at any time of the day.

According to Duffie and Beckman (2009), the position of the Sun at any time of the day can be predetermined, considering the date and geographic location of the viewing point. With this mathematical algorithm the set point signals for the elevation axis and the azimuth axis are generated.

The proposed control strategy is of the open loop type where signals are generated that allow the activation of the two direct current motors, one for elevation movement (0 to 90 °) and the other for azimuth movement (0 to 180 °). , so that to obtain a degree of movement in each axis of rotation, the corresponding motor must give half a revolution. The block diagram of the control system is shown below in Figure 6.

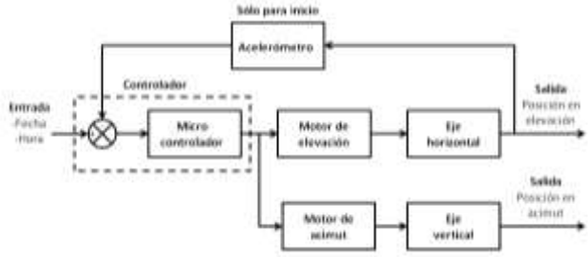


**Figure 6** Control system block diagram.

The controller is the module where all the control and power electronics necessary to obtain a response from the tracking system are located, it is here where the aforementioned mathematical algorithm is housed. Physically it is a micro controller with its own software in conjunction with a minimum power system necessary for its operation. The choice of this microcontroller lies in its large memory capacity and processing speed, sufficient to carry out the trigonometric operations characteristic of the equations that determine the apparent motion of the Sun.

Obtaining the degrees of movement for the positioning of the concentrator, a core part of the microcontroller's programming, starts from the establishment of the date, time, longitude and latitude entries of the geographical place where the concentrator is installed for later perform the corresponding calculations and send two activation signals to a dual type motor speed control card, this in order to reverse the polarity of the motors so that they can be driven in both directions of rotation. This card is the one that ultimately turns the motors for elevation and azimuth on or off.

The accelerometer only acts when the system is actuated for the first time in order to establish the concentrator in a reference point and from there perform the calculations of the rotation in elevation, or when the system must be reset after a failure stop or maintenance.

ISSN 2524-2121

The control system will ensure that the action of the motor is a gradual movement making the output values of the positioning calculations in elevation and azimuth of the Sun be geometrically reproduced as best as possible. Because the apparent movement of the Sun makes a change of approximately 15 ° every hour (Wieder, 2003), the tracking system does not make a continuous movement, instead it generates a change in the position of the concentrator every 5 min.

## Results

Two experimental tests were carried out in the same geographical area under similar weather conditions, test 1 - cloudy weather, test 2 - partially cloudy weather, this by comparing the components of the total radiation that indicates a predominance of diffuse radiation over radiation. direct.

The measurement of the total radiation on a horizontal surface is carried out by means of a total radiation meter in W / m2, calibrated for the solar spectrum under normal test conditions, that is, spectrum for an air mass of 1.5, with GT = 1000 W / m2 at 25ºC, which is similar to direct sunlight at noon in central Europe. From this measurement of total radiation, the direct radiation normal to the concentrator aperture plane was obtained, from the mathematical model of the Erbs correlation (Erbs D. G., Klein S. A., & Duffie J. A., 1982).

From the radiation measurements, an estimate of the incident direct solar radiation is obtained normal to the concentrator aperture plane, from which the absorbed flux at the focal point is calculated, which in turn will serve for future estimates. useful energy which may be subject to experimental verification.

The temperature reached on the absorber element is monitored by a type J, class 2 thermocouple, calibrated for a temperature range from -40 to 750 ºC. The thermocouple at all times remains in direct contact with the absorber element without the latter having any type of thermal insulation.

Considering the experimental data, Graphs 2 and 3 clearly show a linear or proportional relationship between the total radiation and the temperature reached by the absorber at the focal point.

The peaks indicate sampling points that can be considered as instants of solar clarity, it is at these points where the maximum temperature values are reached. However, the abrupt decreases of the same are translated not only as instants where the cloud cover interferes with the passage of solar radiation but also there is the existence of air currents that accelerate the transfer of heat by convection generating heat losses in the absorber element.

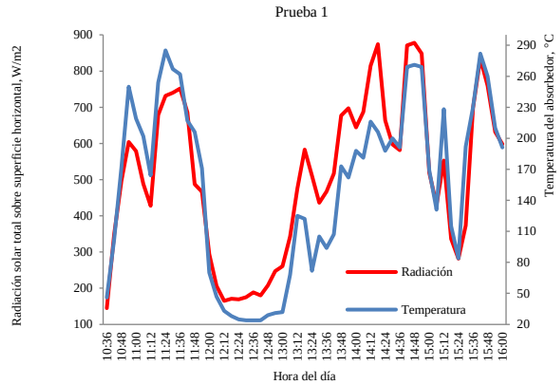


**Graphic 2** Graph of experimental data obtained for test 1.

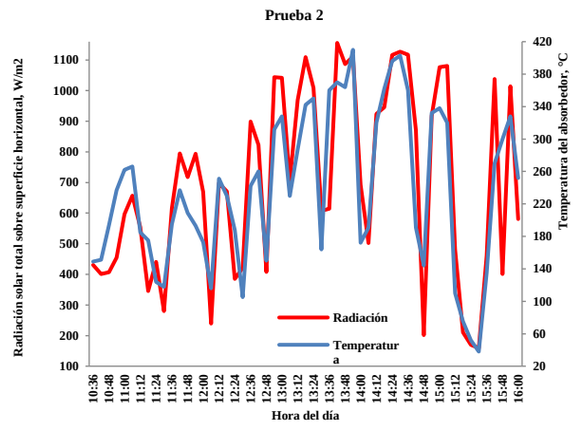


**Graphic 3** Graph of experimental data obtained for test 2.

Taking an average of the maximum and minimum temperature values reached in the collector absorber element, it is considered that in the tests the minimum temperature reached was 24 ° C between 12:30 and 12:42 hrs, while the maximum was 410 ° C at 1:54 PM, under partly cloudy sky conditions.

Currently the solar concentrator is in the experimentation stage with fluid loading, passing through its focal point a thermal oil whose boiling point is 300 ° C.

ISSN 2524-2121

Although improvements are still being implemented in the fluid circulation system, some experimental values from preliminary tests show that the operation of the concentrator for 3 hours increases the temperature of the thermal oil from 26 ° C to 120 ° C, as shown in the Graph 4.

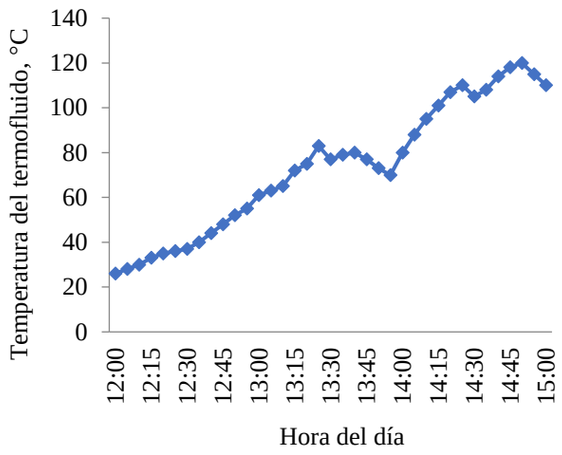


**Graphic 4** Experimental data obtained by circulating thermal oil through the concentrator.

## Acknowledgments

To CONACyT for the financial support provided to the thesis student of the IPN doctoral program.

To the National Polytechnic Institute for the financial support granted in institutional research projects as of 2010.

## Conclusions

From the information resulting from the experimental tests and the calculations obtained from them, it can be concluded that the PDR solar concentrator is functional and fully complies with the proposed objective, being applied on a smaller scale than usual, so that it can be installed in home or small business.

Choosing the right diameter depends in the first instance on knowing the edge angle that provides the maximum concentration. Once known, this angle must be kept constant to ensure maximum concentration and then the most convenient dimensions of focal length and diameter of the disk can be freely varied.

The direct solar radiation incident perpendicular or normal to the aperture plane is at all times greater than the direct radiation on a horizontal plane, this shows that the proposed control system works and that the trajectory of the apparent movement of the Sun is effectively being followed. The system will be positioned in the direction of the Sun regardless of the obstruction of solar radiation, whether by cloud cover, buildings, trees or any other object that generates shade.

The angular scattering error considered allowed dimensioning a suitable focal image width so that the solar radiation reflected by the disk is concentrated almost entirely within the absorbing area. Even so, the concentrator exhibits movement oscillations in its support structure mainly due to the torque applied by the motors at the beginning of each position change.

The minimum and maximum values of temperature reached in the absorber are directly associated with the minimum and maximum of incident solar radiation registered in the radiation meter. Therefore, it can be mentioned that the focal point has a behavior in real time that depends for the most part on the incident solar radiation.

It can be estimated that the operating range of the concentrator shows a wide range of application due to the temperatures that can be reached, registering temperature ranges of more than 400 ° C above the focal point, which makes the concentrator a source of energy of high quality according to the general objective of this study. Therefore, the prototype has a great capacity to be exploited scientifically and commercially due to its simplicity in handling, small modularity and, above all, its great capacity to generate high-quality thermal energy.

There are times when the temperature curve is above the radiation curve, meaning that the absorbing element obtains energy from a different source than the radiation reflected by the parabolic disk.

ISSN 2524-2121

One possible explanation is that there is solar radiation that reaches the absorber from its back and at the same time receives energy by conduction heat transfer from its support device which is made of aluminum and is also exposed to solar radiation, then the sum of these two sources of energy and the low or almost zero speed of the wind so that the absorbing element gives up heat slowly contribute to the fact that at times the heat energy of said element is greater than that provided by the incident solar radiation reflected on the Focal point.

Based on the experimental data obtained by circulating the thermal oil through the concentrator, some preliminary calculations indicate that it could be achieved by increasing a temperature delta of 25 to a mass of water of 100 kg, or generating 30 kg of saturated steam. of water starting from water at 25 ° C.

## References

Duffie, J. A. & Beckman, W. A. (2009). *Solar engineering of thermal processes.* Estados Unidos: John Wiley & Sons, Inc.

Durán, P. (2012). *Diseño y construcción de un prototipo de concentrador solar parabólico de disco reflector para generación de energía térmica*. (Tesis inédita de maestría). Instituto Politécnico Nacional, México, D.F.

Erbs, D. G., Klein, S. A., & Duffie, J. A. (1982). Estimation of the diffuse radiation fraction for hourly, daily, and montly-averange global radiation. *Solar Energy* 28, 293.

Kalogirou, S. Solar energy engineering processes and systems, *Parabolic Dish Reflectors (PDRs)* (pp. 147 – 148). Estados Unidos: Academic Press.

Perales, T. (2007). *Guía del instalador de energías renovable*. México: Limusa.

W. Stine, W. (1985). *Solar energy fundamentals and design with computer applications*. Estados Unidos: John Wiley & Sons, Inc.

Wieder, S. (2003). *An introduction to solar energy for Scientists and Engineers*. Estados Unidos: John Wiley & Sons, Inc.

ISSN 2524-2121

**Article** **ECORFAN Journal- Taiwan**
June, 2020 Vol.4 No.7 9-17

# Mechatronic system to assist rehabilitation therapies for shoulder and elbow joints: Design, kinematic analysis, building and HMI

# Sistema mecatrónico para ayudar en terapias de rehabilitación para articulaciones de hombro y codo: Diseño, análisis cinemático, construcción e HMI

AGUILAR-PEREYRA, Felipe†, ALVARADO, Jorge, ALEGRIA, Jesús and SOSA, José

*Universidad Tecnológica de Querétaro*

ID 1st Author: *Felipe, Aguilar-Pereyra*

ID 1st Coauthor: *Jorge, Alvarado*

ID 2nd Coauthor: *Jesús, Alegria*

ID 3rd Coauthor: *José, Sosa*

**DOI:** 10.35429/EJT.2020.7.4.9.17 Received March 12, 2020; Accepted June 30, 2020

**Abstract**

This work presents a novel application of a system to assist therapies during upper limb rehabilitation. The design and kinematic analysis of a device proposed is presented. Two mechanisms are driven by only one motor develop circular, arc and linear paths in order to move the shoulder and elbow joints in rehabilitation therapies. The first mechanism M1 position, velocity and acceleration are analyzed and its graphics respect to time are obtained. The main goal is to develop a mechatronic system which help to therapists during shoulder or elbow rehabilitation activities and be able to record the patient movements during the session. The methodology includes the study of art state, biomechanic analysis of shoulder and elbow joints, mechanism type selection and kinematic analysis in MATLAB® and its validation in ADAMS®. The main contribution is the proposal of an easy to use mechanism that develop three paths for upper limb rehabilitation. The amplitude and velocity of movements can be programmed, monitored and registered in a computational system and the information used to improve therapy.

**Mechatronic, Rehabilitation, Shoulder, Elbow**

**Resumen**

Este estudio presenta la novedosa aplicación de un sistema mecatrónico en la asistencia en terapias de rehabilitación de la extremidad superior, así como el diseño y análisis cinemático del modelo propuesto. Dos mecanismos impulsados por un actuador desarrollan trayectorias circulares, lineales y de arco, para la movilización de las articulaciones del hombro y el codo como apoyo en las terapias de rehabilitación. Para el mecanismo M1 se realiza análisis de posición, velocidad y aceleración y se obtienen y validan sus gráficas respecto del tiempo. El objetivo es desarrollar un sistema mecatrónico que ayude a terapeutas durante actividades de rehabilitación de hombro y codo y sea capaz de registrar los movimientos de los pacientes durante la sesión. La metodología incluye un estudio del estado del arte, el estudio biomecánico de las articulaciones del hombro y del codo, la selección del tipo del mecanismo y el análisis cinemático en MATLAB® y su validación en ADAMS®. La mayor contribución es la propuesta de un mecanismo de fácil uso que desarrolla tres trayectorias para la rehabilitación de la extremidad superior. La amplitud y velocidad de movimientos puede ser programada, monitoreada y registrada en un sistema computacional y la información usada para mejorar la terapia.

**Mecatrónica, Rehabilitación, Hombro, Codo**

**Citation:** AGUILAR-PEREYRA, Felipe, ALVARADO, Jorge, ALEGRIA, Jesús and SOSA. Mechatronic system to assist rehabilitation therapies for shoulder and elbow joints: Design, kinematic analysis, building and HMI. ECORFAN Journal-Taiwan. 2020. 4-7: 9-17

† Researcher contributing as first author.

 

## Introduction

The World Health Organization reported in 2006 that an estimated 10% of the world's population lives with some form of disability (WHO, 2006). In Mexico, in the 2010 census produced by INEGI (The National Institute of Statistics and Geography), 5.1% of the population have some kind of disabilities (INEGI, 2010) and 58.3% of them have limitations walking and moving. Number of people with disabilities is increasing mainly due to growth population and aging as well. About 80% of people with disabilities live in developing countries; most of them live in poverty and have difficulty accessing basic health services, including rehabilitation services (WHO, 2006).

CRIQ (Integrated Rehabilitation Center of Queretaro) promotes measures to prevent disabilities, rehabilitation and in achieving the goals of equality and full participation of people with disabilities as well (DIF Queretaro, 2014). CRIQ has manual equipment for physical rehabilitation, Figure 1, which indispensably requires at least one therapist for each patient in rehabilitation. In general, automated equipment for aid limb rehabilitation therapies in health institutions in the Mexican state of Queretaro is scarce, mainly due to high costs. Moreover, it has been found that using robotic systems in rehabilitation therapies respect to manual therapies increase profits because they incorporate intensive tasks and interactive exercises (Burgar, Lum, Shor, & Machiel Van der Loos, 2000)(Heo, Gu, Lee, Rhee, & Kim, 2012). Advanced technology can enrich treatments and can help patients who cannot regularly travel to clinics for treatment; however, this is not superior to traditional treatments and cannot replace therapists (Levanon, 2013).

In this project, design and construction of an automatic system programmed by a therapist, assist patients in circular, linear and rocker movements of upper extremity is proposed. The purpose is to help the patient to mobilize the shoulder and elbow's joints in the amplitudes and speeds indicated in therapy, primarily flexion and extension movements.

**Figure 1** Wheel for shoulder and elbow mobilization (KinesioShop, 2014)

## Background

In early 1980, the "Stanford Robotic Aid Project" Professor Bernard Roth Stanford and Inder Perkash, head of "VA Spinal Cord Injury Service" were co-investigators with professors Leifer Dr. Vernon Fickle, the proposed rehabilitation engineering whose goal was to develop a simple general purpose system that could assist individuals with disabilities to achieve independence in activities of daily living (ADLs, activities of daily living) (Burgar et al., 2000). Two exoskeleton systems were manufactured and joined to produce flexion - extension of the elbow and pronation - supination of the forearm in a slave master system. The movements of the master system were reproduced in the slave system via servo positioning systems. The top view shown exoskeleton developed called MIME, Stanford University (USA) Figure 2.

**Figure 2** Mirror-Image Motion Enabler, MIME (Burgar et al., 2000)

ISSN 2524-2121

In 2011 the "Robotic Arm Skate for Rehabilitation" project, developed in New Zealand (Wong, Jordan, & King, 2011) was presented. The device consists of a robotic skateboard for upper extremity rehabilitation; it is able to perform scheduled tasks on a computer, Figure 3. Four electric motors allow you to perform movements on a flat surface. Computer games based exercises encourage the participation of patients and their progress is monitored on the computer.

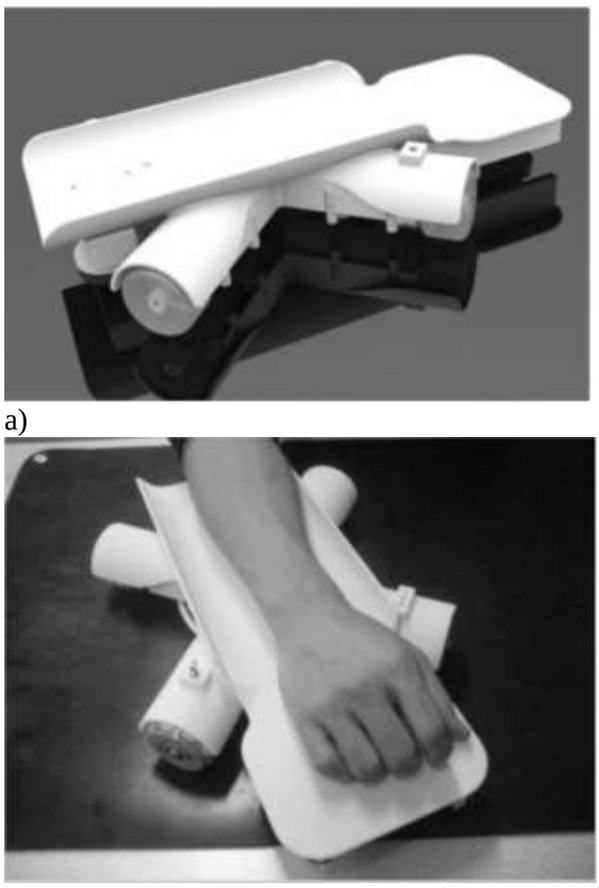

a)

b)

**Figure 3** Robotic Arm Skate for Rehabilitation. a) Platform CAD Design, b) Actual Prototype (Wong et al., 2011)

## Methodology

In the upper extremity rehabilitation, different movements are performed, among the most important circular and linear paths performed with arm and mobilize mainly the shoulder, elbow and wrist mobilization may be found. There are instruments that assist in achieving the mentioned movements; they can be passive or active as shown in Figure 1**.**

## Shoulder Physiology

The shoulder is the proximal joint of upper extremity and is the most mobile of all joints of the human body. Because it has three degrees of freedom, it can guide the upper limb respect to the three planes of space (Kapandji, 2006). In the transverse axis in the frontal plane including B, it allows flexion and extension movements performed in the sagittal plane A. Figures 4 and 5. In the anteroposterior axis, included in the sagittal plane A, allows the movements of abduction and adduction. On the vertical axis, it directs the movements of flexion and extension made in the horizontal plane (cross), with the arm abducted 90 ° (Kapandji, 2006).

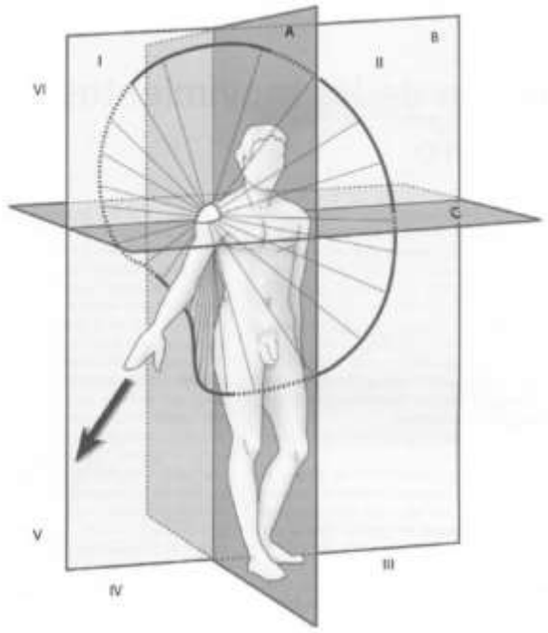


**Figure 4** Body Planes, Sagittal Plane A, Plan B and Plan Front Transverse C. (Kapandji, 2006)

## Elbow flexion-extension

The elbow is the middle joint of the upper extremity, makes the connection between the arm and forearm. Thanks to that achieved by the shoulder orientation can zoom in or out of the body active extremity: the hand (Kapandji, 2006). Anatomically, elbow has only one joint, but the physiology distinguishes two distinct functions: flexion-extension and supination. Elbow's flexion has amplitude of 145 ° maximum, Figure 6.

ISSN 2524-2121

## Design

The Project ―Mechatronic System for Rehabilitation Therapies Shoulder-Elbow Joint Assistance‖, ―SIMATREHC‖ is represented in the block diagram in Figure 7. It consists in a mechatronic system, which has two mechanisms.

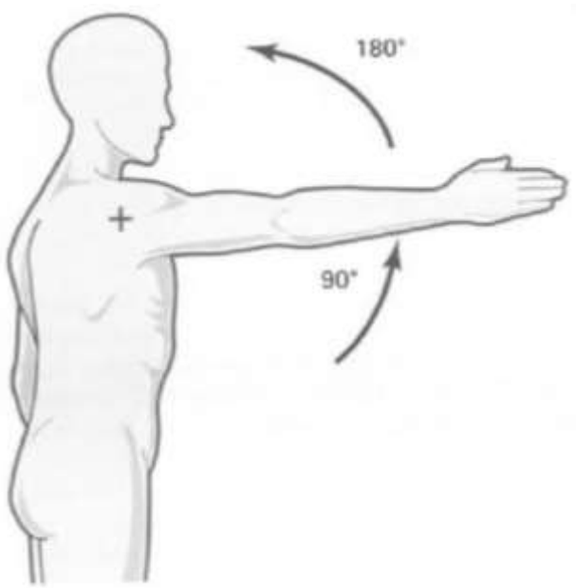


**Figure 5** Shoulder flexion and extension movements performed in the sagittal plane (Kapandji, 2006)

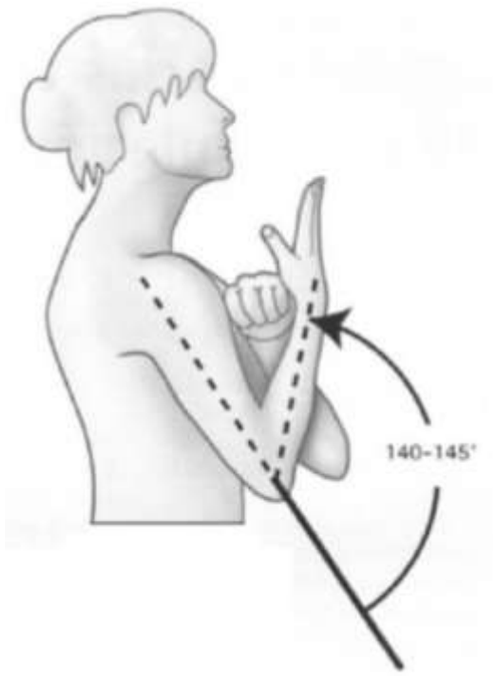


**Figure 6** Elbow flexion-extension movements (Kapandji, 2006)

The slider-crank (R-RRT) type mechanism M1 performs circular paths with adjustable diameter and linear paths for mobilization of the elbow and shoulder mainly.

The four bars mechanism M2 performs rocker or arc paths to mobilize the shoulder. One advantage of the system is that it only requires an electric motor to drive both mechanisms, which generates up to six different movements with two system positions: horizontal and vertical (Sosa et al, 2012.). The engine is controlled by computer equipment through a power amplifier to generate movements with amplitude and speed set in therapy. Subsequently a monitoring and data acquisition will be added to record the performance of each patient rehabilitation sessions.

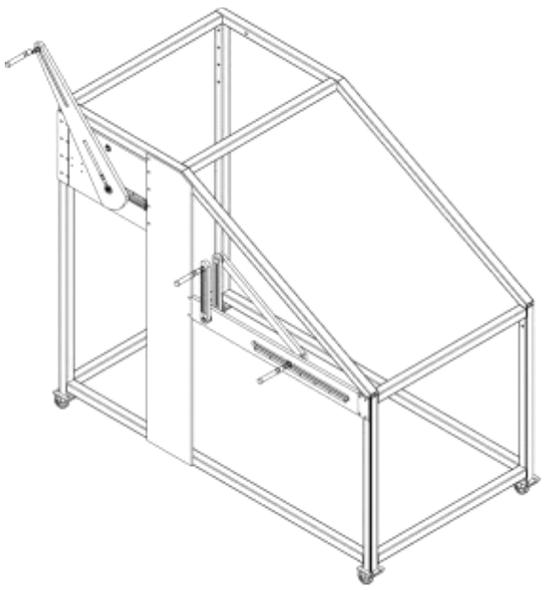

**Figure 7** ―SIMATREHC‖ Project Block Diagram (Aguilar-Pereyra, 2014)

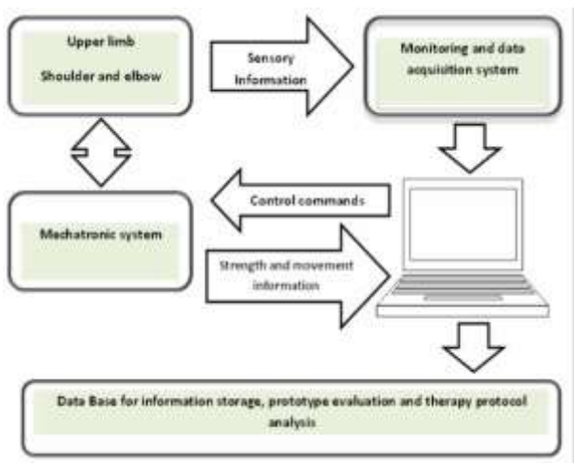


**Figure 8** Complete System

M1

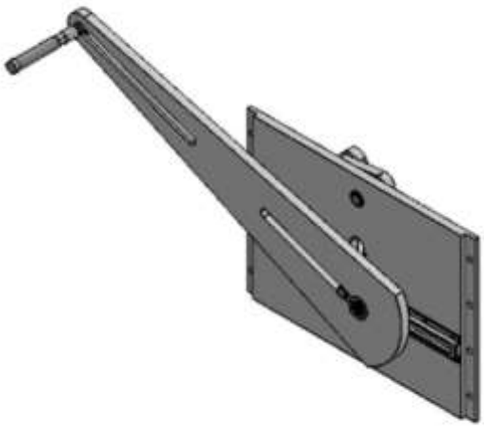

M2

**Figure 9** The crank and slotted lever type mechanism M1. Four bars type M2

Mechanism M1 develops linear and circular paths and has grips that are installed and uninstalled manually according the movement requirements, Figure 9. The mechanism sizes were established based on the anthropometric measurements of the Mexican population (Chaurand Ávila, León Prado, & González Muñoz, 2007).

**Kinematic analysis of mechanism M1**

The kinematic analysis of the mechanism was preformed through vectorial analysis; it computes position (Eq. 2 and Eq. 6), velocity (Eq. 3 and Eq. 7) and acceleration (Eq. 4 and Eq. 8) of the points A and B respectively. Figure 10 shows the front view of the mechanism M1; the driver link 1 is the crank and its dimension is OA. The coupler link dimension is AB and the base link is fixed.

The first step performs a circular movement over point O, so that point A develops circular movement centered at point O and radius OA a path. Point B develops a linear path on the x axis, the amplitude of displacement depends on the angle θ turn the crank and is maximum for θ = π, 2π.

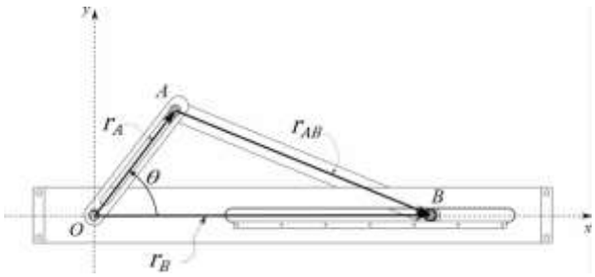


**Figure 10** Front view of mechanism M1

If the links are represented by two-dimensional vectors and a framework **xy** originating at point O is defined because it is fixed, then the position, velocity and acceleration of points A and B are defined by the $\mathbf{r}_A$ and $\mathbf{r}_B$ vectors and their first and second derivatives with respect to time. The A point position is defined by the angle θ:

$$\mathbf{O} = 0\hat{\imath} + 0\hat{\jmath} = (0,0) \quad (1)$$

$$\mathbf{r}_A = x_A\hat{\imath} + y_A\hat{\jmath} \quad (2)$$

$$= L_1\cos\theta\,\hat{\imath} + L_1\,\mathrm{sen}\,\theta\,\hat{\jmath}$$

$$\mathbf{v}_A = \dot{\mathbf{r}}_A = \dot{x}_A\hat{\imath} + \dot{y}_A\hat{\jmath} \quad (3)$$

$$= -L_1\dot{\theta}\,\mathrm{sen}\,\theta\,\hat{\imath} + L_1\dot{\theta}\cos\theta\,\hat{\jmath}$$

$$\mathbf{a}_A = \ddot{\mathbf{r}}_A = \ddot{x}_A\hat{\imath} + \ddot{y}_A\hat{\jmath} \quad (4)$$

$$= (-L_1\ddot{\theta}\,\mathrm{sen}\,\theta - L_1\dot{\theta}^2\cos\theta)\hat{\imath}$$

$$+(L_1\ddot{\theta}\cos\theta - L_1\dot{\theta}^2\,\mathrm{sen}\,\theta)\hat{\jmath}$$

where L1 is the magnitude of the vector rA, is the angular velocity and is the angular acceleration.

Because the movement of point B is along axis **x** and the length of vector $\mathbf{r}_{AB}$ is constant, the component of point B in axis **y** is cero and its position, velocity and acceleration are:

$$(x_B - x_A)^2 + (y_B - y_A)^2 = AB^2 \quad (5)$$

$$\mathbf{r}_B = x_B\hat{\imath} + y_B\hat{\jmath} \quad (6)$$

$$= \left(x_A + \sqrt{AB^2 - y_A^2}\right)\hat{\imath} + 0\hat{\jmath}$$

$$\mathbf{v}_B = \dot{\mathbf{r}}_B = \dot{x}_B\hat{\imath} + \dot{y}_B\hat{\imath} \quad (7)$$

$$= \left(-L_1\dot{\theta}\,\text{sen}\,\theta + L_1\,\omega_2\,\text{sen}\,\theta\right)\hat{\imath} + 0\hat{\jmath}$$

$$\mathbf{a}_B = \ddot{\mathbf{r}}_B = \ddot{x}_B\hat{\imath} + \ddot{y}_B\hat{\jmath} = \quad (8)$$

$$\left(-\ddot{\theta}_1 L_1\,\text{sen}\,\theta - L_1\dot{\theta}^2\cos\theta + \alpha_2 L_1\,\text{sen}\,\theta - \omega_2^2\sqrt{AB^2 - y_A^2}\right)\hat{\imath} + 0\hat{\jmath}$$

where:

$$\omega_2 = \frac{-L_1\dot{\theta}\cos\theta}{\sqrt{AB^2 - y_A^2}} \quad (9)$$

$$\alpha_2 = \quad (10)$$

$$= \frac{-L_1\ddot{\theta}\cos\theta + L_1\dot{\theta}^2\,\text{sen}\,\theta - L_1\,\omega_2^2\,\text{sen}\,\theta}{\sqrt{AB^2 - y_A^2}}$$

## Results

Because the movement of point B is along axis **x** and the length of vector **r**AB is constant, the component of point B in axis **y** is cero and its position, velocity and acceleration are: Design of mechanisms M1 and M2 are presented in Figure 9. Figure 11 shows the kinematic simulation results in MatLab® of movement equations for points A and B of mechanism M1, with lengths OA = 301 mm and AB = 625 mm~~, circular~~ and lineal paths are developed. Results of position, velocity and acceleration simulation of points A and B for constant angular velocity ω= π rad/s in driver link 1 are shown in figures 12 and 13.This results have been validated with the program Adams® with the model developed in Solidworks®.

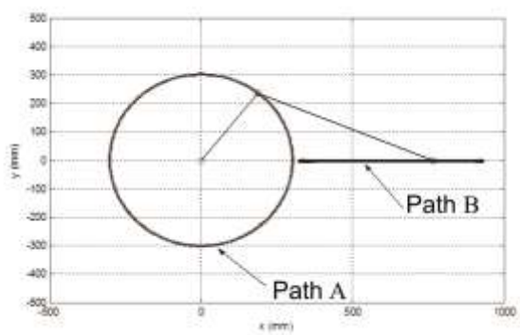


**Figure 11** Simulation results in MatLab® of mechanism

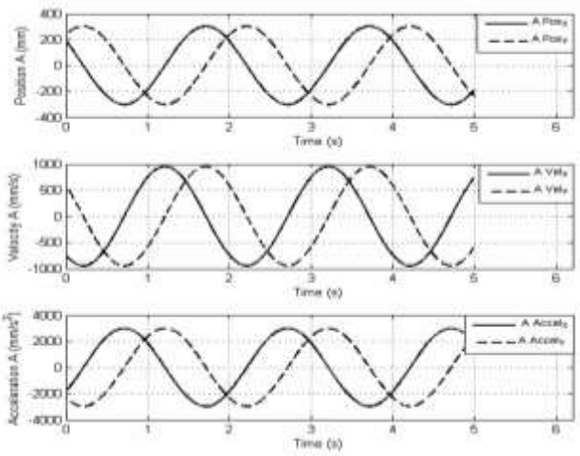

**Figure 12** Simulation results in MatLab® of position, velocity and acceleration of point A of mechanism M1

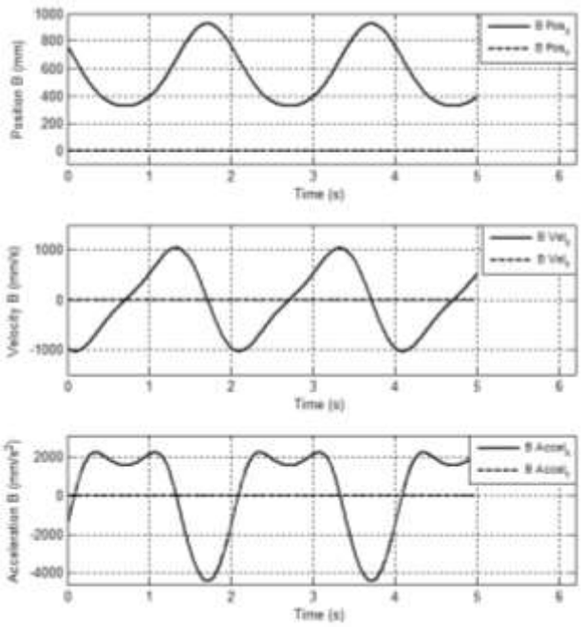

**Figure 13** Simulation results in MatLab® of position, velocity and acceleration of point B of mechanism M1

## Interface for programming and monitoring

The movements of mechanism are programmed by therapist through of an interface. Single movements can be executed in mode jog, a velocity limited has been established. The interface allows execute repetitive movements with amplitude, velocity and number of repetitions established previously. Figure 14 shows the human-mechanism interface developed in software LabVIEW®.

**Figure 14** Interface for programming and monitoring developed in LabVIEW®

The user interface for mechanism control has three displays, through of that user, who can be medic or therapist, sets the values of parameters for mechanism movements. The user can observe the development of mechanism in a display for monitoring. Three aspects of this rehabilitation system development are, in importance order, safety, efficacy and efficiency.

The user interface has three operation modes: Configuration, Teaching and Programming. In Configuration mode, parameters for digital communication between computer and control system are set. Test of performance and safety and movements monitoring can be executed to evaluate limit switch and emergency stop. Functions for Teaching and Programming modes are shown in Table 1 and Table 2.

| Teaching |
|---|
| Manual setting of current position |
| Setting of velocity for manual movement |
| Recording current position in registers |
| Cleaning position registers |
| Editing position registers |
| Turning on and off digital outputs (O1,O2) |
| Setting virtual limit for movements |
| Setting home position |
| Key ―Play‖ for intentional execution |
| Recording movements graph |
| Recording movements data file |
| Emergency Stop routine |

**Table 1** Functions for Teaching mode

| Programming |
|---|
| Setting movements sequences among positions |
| Beginning of movements at home position |
| Selection of positions from registers |
| Setting velocity for single movement |
| Setting time pause between movements |
| Turning on and off digital outputs (O1,O2) |
| Selection step by step or continuous mode |
| Forward or backward sequences execution |
| Key ―Play‖ for intentional execution |
| Recording of graphic of movements |
| Recording of movement file |
| Emergency Stop routine |

**Table 2** Functions for programming mode

## Safety functions for operation of mechanism

―Home‖Position: the initial position of mechanism should be at middle point of full range movement. This position, defined as ―Home‖, corresponds to neutral position, in which flexors and extensors muscles activity is lowest.

Intentional Execution: to be able for moving the mechanism or turning on digital outputs of the system is indispensable to enable key ―Play‖ simultaneously with the other function, it is to avoid accidental activation.

For example, for manually moving the mechanism, is necessary to turn the position control knob simultaneously with key ―Play‖activation. This action can be described by Eq. (11).

$$FunPosition = CPosition \cdot Play \tag{11}$$

where:

FunPosition is the function that sends the movement command to the motor driver.

CPosition is the virtual knob in the user interface which set the value of reference position for mechanism motor.

Play is a virtual key knob in the user interface which takes boolean values.

Functions that require intentional execution are: CPosition, CVelocity, Save, Reset and Turning on and off digital outputs.

ISSN 2524-2121

Emergency Stop: when a virtual or real emergency stop button is activated, the emergency routine is executed, the mechanism movement is stopped and digital outputs are turned off. The emergency stop button is retentive and causes a fault in the system when is activated. This fault is eliminated by sequential activation of keys ―Play‖ and ―Clear‖.

**Functions of Teaching mode**

Manual setting of current position: Cposition knob set the value of reference for the angle of link 1 respect to ―Home‖ position; it is an intentional function. If the position of knob was lower than the virtual LowerLimit or upper than UpperLimit, the value of Cposition will take the value of the virtual LowerLimit or UpperLimit.

Setting of velocity for manual movement: the slider CVelocity establish the value of highest velocity for mechanism movements, the range is from 0-100% of motor highest absolute velocity; this function is intentional.

Recording current position in registers: the current position value, including initial position, is saved into a register by pressing key ―Save‖. The value of knob CPosition is recorded in a register of position array, the index begins in zero and increments its value every time that key ―Save‖ is pressed; this function is intentional.

Cleaning position registers: when key ―Reset‖ is pressed, all the array of position registers is saved with zeros, a zero is saved to the Index; this function is intentional.

Editing position registers: to change the value of a position register is necessary to select the value of ―Index‖ that corresponds to desired register using keys ―Prev‖ and ―Next‖, finally pressing key ―Save‖ and the new position value is recorded.

Turning on and off digital outputs (O1, O2): to set or reset digital outputs is necessary to activate the key that corresponds; previously key ―PLAY‖ should be activated because this function is intentional

Setting virtual limit for movements: to set virtual limits of movement, that are different of absolute limits, values for controls LOWERLIMIT and UPPERLIMIT should be established. This is a preventive action to configure movements in a smaller range tan full range. Recording movements graph: this function saves an image file of movements.

Recording movements data file: this function saves a text file of movements, it includes time, position and velocity for each sample. This function is executed automatically by pressing key ―STOP‖.

Finally, Figure 15 shows prototype built, it corresponds to Figure 8.

**Figure 15** Prototype

**Conclusions**

Application of mechatronic systems can supply external forces for limbs mobilization in rehabilitation therapies; it cannot substitute human therapist in none case, moreover this kind of systems should be used under strict professional supervision. The proposed system allows three different movements with only one motor, which supplies the strength for controlled movements in position, velocity, acceleration and iterations. This Project has a wide scope, actual status, presented here, includes design and kinematic analysis of mechanism M1. Mechanisms design is based on movements with circular, linear and arch paths and the anthropometric measurements of the Mexican population. Mechanisms can be adjusted to different zises of shoulder and elbow. Future work includes dynamic analysis for torque required in motor, instrumentation for strength measuring and the full system evaluation.

ISSN 2524-2121

**Acknowledges**

This work is financially supported by ―Programa para el Desarrollo Profesional Docente‖ by S.E.P. México. The authors also like to acknowledge the CRIQ therapists for their advice for problem identification.

**References**

Aguilar-Pereyra Felipe et al., Sistema Mecatrónico para Asistencia en Terapias de Rehabilitación de las Articulaciones Hombro – Codo: Diseño y Análisis Cinemático. I Congreso nternacional de Investigación y Redes de Colaboración, UTEQ 2014.

Ávila Chaurand, R., Prado León, L. R., & González Muñoz, E. L. (2007). Demensiones antropométricas Población Latinoamericana. (U. de Guadalajara, Ed.) (2da ed., p. 280). Guadalajara: Universidad de Guadalajara.

Burgar, C. G., Lum, P. S., Shor, P. C., & Machiel Van der Loos, H. F. (2000). Development of robots for rehabilitation therapy: the Palo Alto VA/Stanford experience. Journal of Rehabilitation Research and Development, 37(6), 663–73. Retrieved from http://www.ncbi.nlm.nih.gov/pubmed/11321002

DIF Querétaro. (2014). CRIQ. Retrieved from www.queretaro.gob.mx/dif/programas.aspx?q=63j01wSCoaxjH1pHefrcxA%3D%3D

Heo, P., Gu, G. M., Lee, S., Rhee, K., & Kim, J. (2012). Current hand exoskeleton technologies for rehabilitation and assistive engineering. International Journal of Precision Engineering and Manufacturing, 13(5), 807–824. doi:10.1007/s12541-012-0107-2

INEGI. (2010). Las personas con discapacidad en México , una visión al 2010. (Instituto Nacional de Estadística y Geografía (México). Ed.) (2010th ed., p. 272). México.

Kapandji, A. I. (2006). Fisiología articular: esquemas comentados de mecánica humana. (Editorial Médica Panamericana, Ed.) (6th ed., p. 349). Madrid.

KinesioShop. (2014). Productos para Rehabilitación y Kinesiología.

Levanon, Y. (2013). The advantages and disadvantages of using high technology in hand rehabilitation. Journal of Hand Therapy : Official Journal of the American Society of Hand Therapists, 26(2), 179–83. doi:10.1016/j.jht.2013.02.002

WHO. (2006). Disability and rehabilitation. World Health Organization. Retrieved from http://www.who.int/nmh/donorinfo/vip_promoting_access_healthcare_rehabilitation_update.pdf.pdf

Wong, C. K., Jordan, K., & King, M. (2011). Robotic arm skate for stroke rehabilitation. IEEE. International Conference on Rehabilitation Robotics : [proceedings], 2011, 5975389. doi:10.1109/ICORR.2011.5975389

Sosa Josemaría, Ortiz Tania, Aguilar-Pereyra Felipe, Memoria Sistema mecatrónico para asistencia en terapias de Rehabilitación de la articulación hombro-codo en la Extremidad superior. UTEQ. 2014.

ISSN 2524-2121

**Article** **ECORFAN Journal- Taiwan**
June, 2020 Vol.4 No.7 18-27

# Image resolution enhancement via sparse interpolation on wavelet domain

# Mejora de la resolución de la imagen mediante interpolación escasa en el dominio de ondículas

CHAVEZ, Román†, PONOMARYOW, Volodymyr and CASTRO, Fernando

*Universidad Tecnológica de la Región Norte de Guerrero, Iguala, Gro.*

ID 1st Author: *Román, Chavez*

ID 1st Coauthor: *Volodymyr, Ponomaryow*

ID 2nd Coauthor: *Fernando, Castro*

**DOI:** 10.35429/EJT.2020.7.4.18-.27 Received March 22, 2020; Accepted June 30, 2020

**Abstract**

The image processing algorithms collectively known as super-resolution (SR) have proven effective in producing high-quality imagery from low-resolution (LR) images. This paper focuses on a novel image resolution enhancement method employing the wavelet domain techniques. In order to preserve more edge information, additional edge extraction step is proposed employing high-frequency (HF) sub-band images - low-high (LH), high-low (HL), and high-high (HH) - via the Discrete Wavelet Transform (DWT). In the designed procedure, the LR image is used in the sparse interpolation for the resolution-enhancement obtaining low-low (LL) sub-band. Additionally, all sub-bands (LL, LH, HL and HH) are performed via the Lanczos interpolation. Finally, the estimated sub-band images are used to form the new high-resolution (HR) image using the inverse DWT (IDWT). Experimental results on real data sets have confirmed the effectiveness of the proposed framework in terms of objective criteria as well as in subjective perception.

**Super-resolution, Wavelet-domain, Sparse interpolation**

**Resumen**

Los algoritmos de procesamiento de imágenes colectivamente conocidos como súper-resolución (SR) han demostrado ser eficaces en la producción de imágenes de alta calidad a partir de imágenes de baja resolución (LR). Este artículo se centra en un método de mejora de la resolución de imagen novedosa que emplea las técnicas de dominio wavelet. Con el fin de preservar más la información de bordes, adicionalmente se propone una etapa de extracción de bordes que emplea altas-frecuencias (HF) en la sub-banda de las imágenes – pasa-alta (LH), pasa-baja (HL), y alta-alta (HH) - a través de la Transformada Discreta Wavelet (DWT). En el procedimiento diseñado, la imagen LR se utiliza en la interpolación sparse para el mejoramiento en la resolución de la sub-banda baja-baja (LL). Además, todas las sub-bandas (LL, LH, HL y HH) se realizan a través de la interpolación Lanczos. Finalmente, las imágenes de las sub-bandas son usadas para formar la nueva imagen de alta resolución (HR) mediante la DWT inversa (IDWT). Los resultados experimentales en conjuntos de datos reales han confirmado la eficacia del marco propuesto en términos de criterios objetivos, así como en la percepción subjetiva.

**Súper-resolución, Extracción de bordes, Dominio wavelet, Interpolación sparse**

**Citation:** CHAVEZ, Román, PONOMARYOW, Volodymyr and CASTRO, Fernando. Image resolution enhancement via sparse interpolation on wavelet domain. ECORFAN Journal-Taiwan. 2020. 4-7: 18-27

† Researcher contributing as first author.

 

## Introduction

Relatively recently, researchers have begun developing methods to extend the SR algorithms to different imaging applications. There are differences that depend of imaging applications. Medical imaging applications differ from photographic imaging in several key respects. Unlike photographic imaging, medical imaging applications often use highly controlled illumination of the human subject during image acquisition that usually leads to higher signal-to-noise ratios (SNR). On other hand, the image processing artifacts are much less tolerable in medical images than in photographic applications. Another difference is that the majority of medical imaging applications involve creating images through three-dimensional objects. Thus, while the final images are two dimensional, they represent some form of projection through a three-dimensional volume [1].

The general image capture model, or forward model, combines the various effects of the digital image acquisition process such as point-wise blurring, motion, under-sampling, and measurement noise. The problem in this point is to estimate an HR image *u(m,n)* from measurements of an LR image *f(m,n)* that were obtained through a linear operator *K* that forms a degraded version of the unknown HR image, which was additionally contaminated by an additive noise , and can be represented as the forward imaging model as follows:

$$f(m,n) = K[u(m,n)] + \mathcal{E}(m,n). \quad (1)$$

In most applications, *K* is a subsampling operator that should be inverted to restore an original image size and this problem usually should be treated as an ill-posed problem. Many image display devices have zooming abilities that interpolate input images to adapt their size to HR screens. Current proposal introduces a general class of nonlinear inverse estimators that were obtained with an adaptive mixing of linear estimators, with applications to image interpolation. Wavelets also play a significant role in many image processing applications. The 2-D wavelet decomposition of an image is performed by applying the 1-D DWT along the rows of the image first, and then, the results are decomposed along the columns.

This operation results in four decomposed sub-band images. The frequency components of those images in the sub-bands cover the full frequency spectrum of the original image. Image resolution enhancement using wavelets is a relatively new subject, and recently, many novel algorithms have been proposed [2-6]. These algorithms have attempted to improve the sharpness and fine features by using special procedures in the wavelet domain; where such reconstructions are performed by manipulations in the different decomposition sub-bands.

Prior information on the image sparsity has been widely used for image interpolation [7]. Wavelet estimators were introduced to compute fine-scale wavelet coefficients by extrapolating larger-scale wavelet coefficients [8, 9]. A more general and promising class of nonparametric SR estimators assumes that the HR image *u(m,n)* is sparse in some dictionary of vectors. This sparse representation is estimated by decomposing the LR measurements *f* in a transformed dictionary [10, 11]. The principal idea behind the restriction of the sparse SR algorithms is that the HR results can be improved by using more prior information on the image properties. The predominant task of current study is consists of using an approach based on wavelet decomposition techniques that permit to take into account both spatial and spectral wavelet pixel information to enhance the resolution of a single image that can also be expanded to video sequences of different types [12, 13].

The principal contributions of current SR proposal in difference to other state of-the-art resolution-enhancement techniques consists in the mutual interpolation via *Lanczos* and Nearest-neighbor interpolation (*NNI)* techniques employed in *Wavelet Transform* (WT) HF sub-band images, an edge extraction procedure in wavelet transform space and adaptive directional LR image interpolation via sparse image mixture models in a DWT frame. The proposed framework additionally applies special denoising filtering that uses the *Non-Local Means* (NLM) for the input LR image performing better robustness in the SR process. Finally, all of the sub-band images are combined, generating a final HR image via IDWT that presents better resolution performance in terms of the objective criteria and subjective visual perception in comparison with the best existing algorithms.

ISSN 2524-2121

To justify that the novel algorithm of image resolution enhancement has real advantages, we have compared the proposed SR procedure with other similar techniques, such as the following: Demirel-Anbarjafari Super Resolution (DASR) [14], *Wavelet domain image resolution enhancement using Cycle- Spinning,* (WDIRECS) [15], *Image Resolution Enhancement applying Discrete and Stationary Wavelet Decomposition (IREDSWD) [16], and Discrete Wavelet Transform-Based Satellite Image Resolution Enhancement (DWTSIRE) [17]*. To ascertain the effectiveness of the proposed algorithm over other wavelet-domain resolution enhancement techniques, different LR images of different nature (satellite, medical and optical) obtained from [18, 19] were tested. The first database consists of the 20 medical images, and the second database contains 38 satellite images. All images have format of 8 bits/pixels for gray scale.

The remainder of this paper is organized as follows. Section 2.1 presents a short introduction to the NLM filtering method, Section 2.2 shows an implementation of an image interpolation through the inverse mixing estimator in a single image in wavelet space. The proposed technique for image SR reconstruction is presented in Section 3. Section 4 explains the applied quality criteria that were used to quantify the SR results. Section 5 discusses the qualitative and quantitative results of the proposed technique in comparison with other better conventional techniques. Finally, the conclusions are drawn in the final section.

**Problem statement proposed methodology**

**Non-Local Means Filtering**

The NLM algorithm computes a denoised pixel $\hat{u}(m,n)$ by applying the weighted mean of the surrounding pixels of $f(m,n) = \{f(r,s)|(r,s) \in N(m,n)\}$, the estimated value for a pixel $(m,n)$, is computed as a weighted average of all the pixels in the image [20]:

$$\hat{u}(m,n) = \frac{\sum_{(r,s)\in N(m,n)} f[r,s]w[m,n;r,s]}{\sum_{(r,s)\in N(m,n)} w[m,n;r,s]}, \quad (2)$$

Where $N(m,n)$ stands for the neighborhood of the pixel $f[r,s]$, and the term $w[m,n;r,s]$ is the weight for the *(m,n)-th* neighbor pixel.

The weights for the filter are computed based on radiometric (grey-level) proximity and geometric proximity between the pixels, namely:

$$w[m,n;r,s] = exp\left\{-\frac{(f[m,n]-f[r,s])^2}{2\gamma^2}\right\} \cdot g\left(\sqrt{(m-r)^2+(n-s)^2}\right). \quad (3)$$

The function $g$ takes the geometric distance into account. The parameter controls the effect of the grey-level difference between the two pixels. This way, when the two pixels that is markedly different, the weight is very small, implying that this neighbor is not to be trusted in the averaging. The denoised image is used in next steps of the proposed framework.

**Interpolations with Sparse Wavelet Mixtures**

The subsampled image $\hat{u}(m,n)$ is decomposed with one level DWT in the sub-bands (LL - approximations; and LH – horizontal details, HL – vertical details, HH diagonal details), which are treated as the matrixes H whose columns (approximations and details) are the vectors of a wavelet frame on a single scale. A construction is performed with a dual frame matrix H whose columns are the dual wavelet frames $\{h_{m,n}\}_{0\le m\le 3}$ [21]. The wavelet coefficients are written as follows:

$$\hat{z}(m,n) = \langle \hat{u}, h_{m,n}\rangle = H\hat{u}(m,n). \quad (4)$$

The WT separates an LF image (an approximation) $z_l$ that is projected over the sub-band image *LL* scaling filters $\{h_{0,n}\}_{n\in\mathcal{G}}$ and an HF image (details) $z_h$ that is projected over the finest scale wavelets *LH, HL,* and *HH* in three directions $\{h_{m,n}\}_{1\le m\le 3, n\in\mathcal{G}}$.

$$z_l = \sum_{n\in\mathcal{G}} \hat{z}(0,n)h_{0,n} \quad and \quad z_h = \sum_{m=1}^{3} \hat{z}(m,n)h_{m,n}. \quad (5)$$

The LF image $z_l$ has little aliasing, and it can be interpolated sufficiently well when applying a *Lanczos* interpolator $V^+$. For interpolating the HF image $z_h$, we employ directional interpolators $V_\theta^+$ for $\theta \epsilon \Theta$, where $\Theta$ is a set of angles that is uniformly discretized between 0 and $\pi$.

For each angle $\theta$, a directional interpolator $V_\theta^+$ is applied over a block $D = D_{\theta,q}$ of wavelet coefficients if the directional regularity factor $\|\bar{Q}_D \hat{z}\|$; $\bar{Q}_D$ (sparse regularity operators) is relatively small in the mentioned block. Such regularization is effective if the eigenvalues of the self-conjugated operator $\bar{Q}_D^* \bar{Q}_D$ have an overall variation that is sufficiently large to distinguish regular variations from non-regular variations in a given direction $\theta$ in $D$. For this step, it was proposed to choose rectangular blocks $D = D_{\theta,q}$ that are elongated in the direction of $\theta$. Each block $D$ in the spatial neighborhood of $q$ is chosen to be identical in the three bands $d = 1,2,3$; thus, $l_D(m,n) = l_D(m)$, where $l_D$ is the indicator of the approximation set $D$.

Each image $\hat{z}_D$ that is reconstructed from fine-scale wavelet coefficients in a block $D = D_{\theta,q}$ is interpolated with a directional interpolator $V_D^+ = V_\theta^+$. The HF residual $\hat{z}_r$ and the image LF $f_l$ are interpolated with a separable and nearly isotropic *Lanczos* interpolator $V^+$. The resulting interpolator can be written in the following form [22]:

$$U_{LL} = V^+ \hat{z}(m,n) + \sum_{\theta \epsilon \Theta} (V_\theta^+ - V^+) \mathrm{R}\left( \sum_{q \epsilon \Omega_\theta} \bar{a}(D_{\theta,q}) l_{D_{\theta,q}} \hat{z}(m,n) \right). \quad (6)$$

The image $\hat{z}(m,n)$ is first interpolated with a separable *Lanczos* interpolator $V^+$. For each angle $\theta$, an update is computed over wavelet coefficients of each block of direction $\theta$ multiplied by their mixing weight $\bar{a}(D_{\theta,q})$, with the difference between the separable interpolator $V^+$ and a directional interpolator $V_\theta^+$ along $\theta$. This overall interpolator is calculated with $O(|\Theta|N)$ operations, where $|\Theta| = 20$ is the number of interpolation angles. Numerical experiments are performed with 20 angles, with blocks having a width of 2 pixels and a length between 6 and 12 pixels depending on their orientation.

**Proposed approach in resolution enhancement**

In this technique, one level of DWT that applies different wavelet families is used to decompose an input image. DWT separates an image into different sub-bands. The interpolation process should be applied to the four sub-band images.

Additionally, the novel framework applies a denoising procedure by using the *Non-Local Means* (NLM) for the input LR image (Noise Reduction Stage, Fig.1). This approach has better performance on the HF image components and generates significantly sharper and clearer edges and fine features in the final SR image.

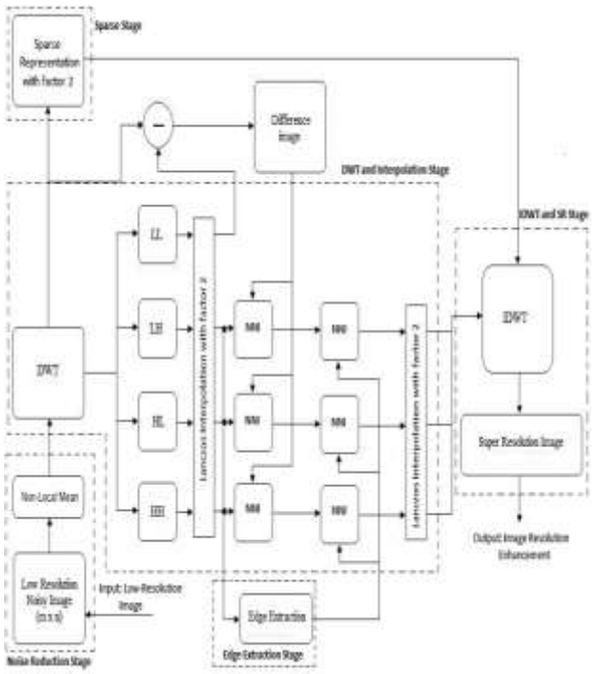


**Figure 1** Block diagram of the proposed resolution-enhancement algorithm

The differences between the interpolated LL sub-band image (with factor 2) and the LR input image are in their HF components that why it has been proposed the intermediate process to correct the estimated HF components applying this difference image. As it is seen in DWT and interpolation stage of the algorithm (Fig.1), this difference is performed in HF sub-bands by interpolating each band via NNI process (changing the values of pixels in agree with the closest neighbor value), including additional HF features into the HF images.

In the proposed SR procedure, the LR image is used as the input data in the sparse representation for the resolution-enhancement process in the following way (Sparse Stage, Fig.1). Finally, the algorithm computes the missing samples along the direction from the previously calculated new samples, where the entire sparse process is performed with the *Lanczos interpolation*, reconstructing LL sub-band. To preserve more edge information and to obtain a sharper enhanced image, we have proposed an extraction step of the edge using

The mean absolute error (MAE) is presented as follows: HF sub-bands images, that employs the first level in the DWT decomposition for an input image LR, the edge information is used into HF sub-bands employing NNI process (Edge Extraction Stage in Fig.1). The edge extracted image is calculated as follows [24]:

$$S = \sqrt{(HH)^2 + (HL)^2 + (LH)^2}, \quad (7)$$

Finally, we perform an additional interpolation with *Lanczos* interpolation (factor 2) to reach the required size for the IDWT process (IDWT and SR Stage, Fig.1). It was noticed that the intermediate process of adding the difference image (the image that contains the HF components) generates a significantly sharper reconstructed SR image. This sharpness is boosted by the fact that the interpolation of the isolated HF components in HH, HL, and LH appears to preserve more HF components than interpolating from the LR image directly.

**Performance evaluation**

In order to evaluate the effectiveness of the proposed resolution enhancement algorithm, the following criteria are employed: peak signal-to-noise ratio (PSNR), mean absolute error (MAE), finally the similarity structural index measure (SSIM) [25, 26] which match better human subjectivity.

The PSNR is defined as:

$$PSNR = 10 \cdot log_{10} \frac{(255)^2}{MSE}, \text{dB}, \quad (8)$$

Where, the mean square error (MSE) is the error measure for a gray scale image of dimension $mxn$.

The mean absolute error (MAE) is presented as follows:

$$MAE = \frac{1}{mxn} \sum_{i=1}^{m} \sum_{j=1}^{n} |\hat{u}[i,j] - u[i,j]| \quad 9)$$

To obtain the objective criteria value, PSNR and MAE employ the reference image (HR) $u(i,j)$ and the reconstructed SR image estimated via the SR algorithm $\hat{u}(i,j)$.

The standard quality metrics used in the past such as PSNR, can be erroneous in some cases; therefore, novel metrics, such as SSIM, which matches human subjectivity better, should be used to characterize the performance of the algorithm. For monochrome images, the SSIM metric values are defined as follows:

$$SSIM(u,\hat{u}) = \left[\frac{2\mu_{\hat{u}}\mu_u + C_1}{\mu_{\hat{u}}^2 + \mu_u^2 + C_1}\right] \cdot \left[\frac{2\sigma_{\hat{u}}\sigma_u + C_2}{\sigma_u^2 + \sigma_{\hat{u}}^2 + C_2}\right] \cdot \left[\frac{\sigma_{\hat{u}u} + C_3}{\sigma_{\hat{u}}\sigma_u + C_3}\right], \quad 10)$$

Here, $\hat{u}$ is the reconstructed SR image, and $x$ is the original (HR) image; $\mu$ and $\sigma^2$ are the sample mean values and sample variances for the $u$ or $\hat{u}$ images, and $\sigma_{\hat{u}u}$ is the sample cross-variance between the $\hat{u}$ and $u$ images. The justification of the SSIM index can be found in [25, 26]. The constants $C_1$, $C_2$, and $C_3$ are used to stabilize the metric for the case in which the means and variances become very small, and usually $C_1=C_2=C_3=1$.

Because it is difficult to define the objective criteria that should be used to ensure the accurate quantization of the reconstructed images, a subjective measure of the image distortion was used in this study via subjective visual perception by human visual system.

A subjective visual comparison of the images provides information about any spatial distortion or artifacts introduced by the algorithm that is employed and, thus, can make it possible to evaluate the performance of the analyzed technique in a different manner.

ISSN 2524-2121

## Experimental results and discussion

In order to show the effectiveness of the proposed method over the conventional and state-of-the-art image resolution enhancement techniques, different test images (*Baboon*, *Elaine*, *Aerial-A*, *Aerial-B*, *Medical-1* and *Medical-2*) with different feature are used for comparison from mentioned image databases.

In this paper, the following families of classic wavelet functions are used: *Daubechies* (Db), *Symlet* (Sym), and *biorthogonal* (Bior). Referring to the image *Baboon (*Fig. 2) shows the results of the SR reconstruction algorithm applied to a LR 128×128 pixels image to obtain a 512x512 pixels resolution enhancement image. The novel resolution enhancement algorithm appears to perform better in terms of objective criteria (PSNR and SSIM) as well as in terms of subjective perception, especially using wavelet *Db-1*. The visual subjective perception can be verified in the zoomed part of the *Baboon* image (left eye), where fine details appear to be preserved better in the novel proposed SR framework.

In the SR reconstructed *Elaine* image, one can observe from analyzing Fig. 3 that the novel algorithm performs better in PSNR and SSIM, especially using wavelet *Sym-2*, also it presents the better perception especially in the well-defined borders (see the zoomed part of the image).

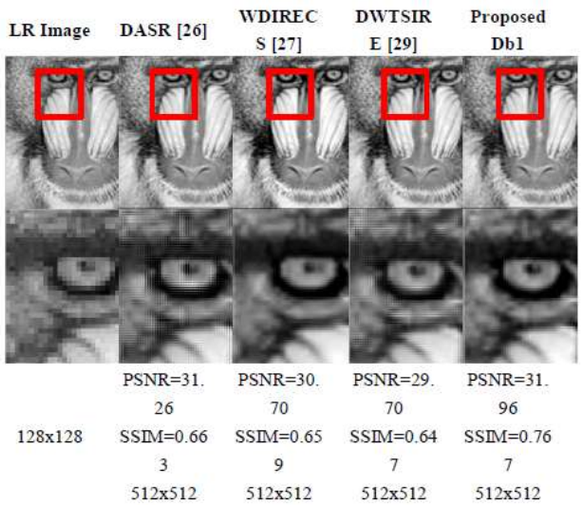


**Figure 2** Visual perception results for the Baboon image contaminated by Gaussian noise (PSNR=17 dB)

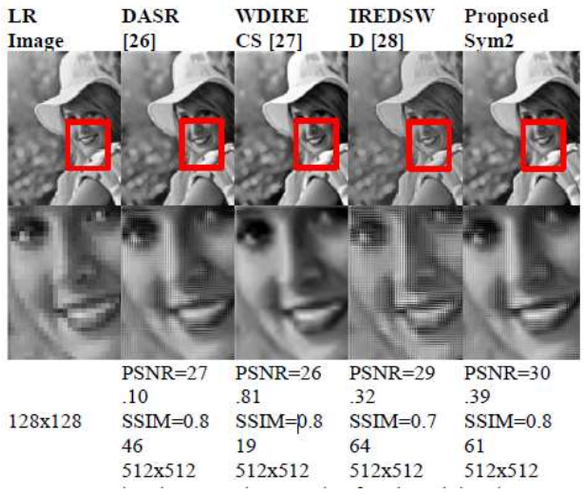


**Figure 3** Visual perception results for the Elaine image contaminated by Gaussian noise (PSNR=17 dB)

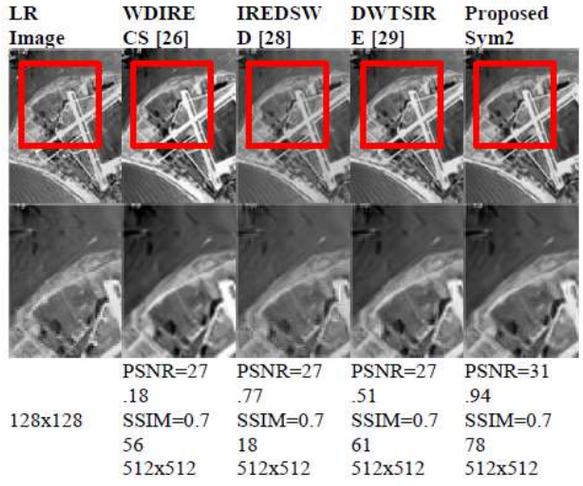


**Figure 4** Visual perception results for the Aerial-A image contaminated by Gaussian noise (PSNR=17 dB)

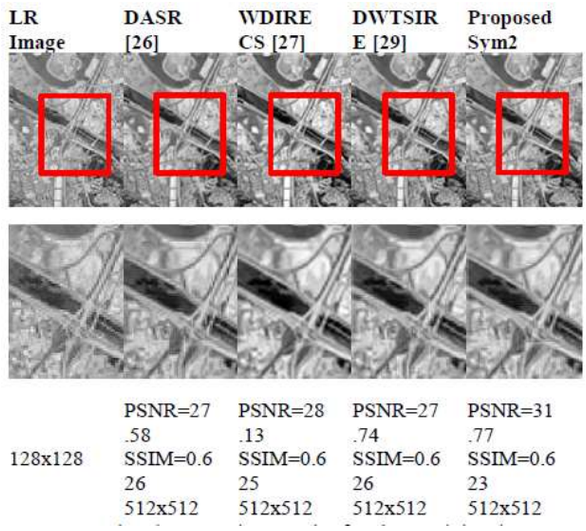


**Figure 5** Visual perception results for the Aerial-B image contaminated by Gaussian noise (PSNR=17 dB)

In the resolution enhancement of the *Aerial-A* image (see Fig. 4), one can observe that there is better performance in terms of the objective criteria PSNR and SSIM as well as in the subjective perception when the proposed SR procedure is employed with the wavelet *Sym-2* in comparison with the other state-of-the art technique.

Fig. 5 compares the *Aerial-B* image obtained by different algorithms. In the zoomed images, one can observe that conventional SR methods produce some blur and artifacts. In contrast, the novel SR algorithm provides better image quality (PSNR and SSIM), when the wavelet *Sym-2* is employed. The proposed SR algorithm restores slightly better regular geometrical structures.

The resolution enhancement algorithms have an important application in the processing of medical images. For this reason, we have tested several medical images. In the *Medical-1* image (see Fig. 6), it is easy to see better performance in accordance with the objective criteria and via subjective visual perception in SR enhancement when the proposed algorithm is employed with the wavelet *Sym-2*. Better preservation of the fine details in the zoomed part of the image can be obtained for the novel resolution enhancement framework.

Fig. 7 compares the SR image *Medical-2* obtained by different algorithms. In the zoomed images, one can observe that conventional SR methods produce some blur and artifacts. In contrast, the novel proposed algorithm provides better image quality (PSNR and SSIM), when the wavelet *Sym-2* is employed. The proposed algorithm restores slightly better regular geometrical structures, as shown in the zoomed part in *Medical-2*.

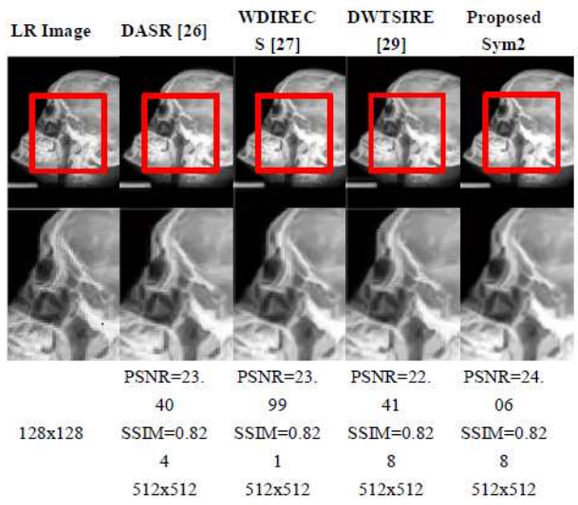


**Figure 6** Visual perception results for the Medical-1 image contaminated by Gaussian noise (PSNR=17 dB)

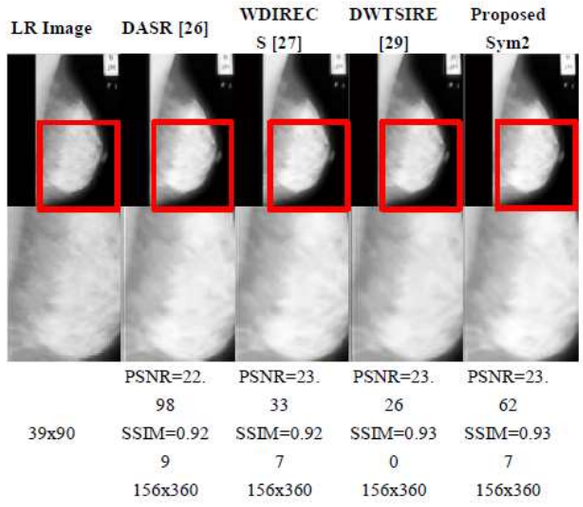


**Figura 7** Visual perception results for the Medical-2 image contaminated by Gaussian noise (PSNR= 17 dB)

In these experiments, we revise the resolution enhancement of a number of images from databases. It can be concluded from this analysis of the SR enhancement images that novel framework results in sharper edges and SR results.

Overall, the results in table 1, 2, 3 and 3 show the better performance in terms of the objective criteria (PSNR, MAE and SSIM) as well as in the subjective perception via human visual system.

ISSN 2524-2121

| SR Methods | | Baboon | | | Elaine | | |
|---|---|---|---|---|---|---|---|
| | | MAE | PSNR | SSIM | MAE | PSNR | SSIM |
| IREDSWD [16] | Db1 | 7.968 | 31.055 | 0.648 | 7.547 | 29.433 | 0.764 |
| | Sym 2 | 7.677 | 30.909 | 0.589 | 7.117 | 29.320 | 0.764 |
| | Bior 1.3 | 9.178 | 30.295 | 0.626 | 8.340 | 28.181 | 0.744 |
| DWTSIRE [17] | Db1 | 8.192 | 29.702 | 0.647 | 8.020 | 26.830 | 0.824 |
| | Sym 2 | 10.864 | 29.450 | 0.640 | 7.481 | 27.625 | 0.861 |
| | Bior 1.3 | 10.967 | 29.288 | 0.532 | 7.207 | 26.982 | 0.786 |
| DASR [14] | Db1 | 6.833 | 31.261 | 0.663 | 7.273 | 26.748 | 0.805 |
| | Sym 2 | 7.325 | 30.985 | 0.647 | 7.986 | 27.106 | 0.846 |
| | Bior 1.3 | 7.191 | 31.158 | 0.654 | 7.557 | 26.745 | 0.804 |
| WDIRECS [15] | Db1 | 7.263 | 30.700 | 0.659 | 7.490 | 26.681 | 0.767 |
| | Sym 2 | 6.260 | 31.357 | 0.657 | 6.199 | 26.814 | 0.819 |
| | Bior 1.3 | 7.244 | 30.709 | 0.659 | 7.554 | 26.667 | 0.766 |
| PROPOSED SR TECHNIQUE | Db1 | **5.412** | **31.968** | **0.767** | 6.951 | 30.256 | 0.835 |
| | Sym 2 | 5.557 | 32.137 | 0.620 | **5.561** | **30.398** | **0.861** |
| | Bior 1.3 | 5.585 | 31.898 | 0.716 | 6.429 | 30.484 | 0.829 |

**Table 1** Objective criteria values of the resolution enhancement from 128x128 to 512x512. (The LR image is contaminated by Gaussian noise PSNR=17 dB)

| SR Methods | | Aerial-A | | | Aerial-B | | |
|---|---|---|---|---|---|---|---|
| | | MAE | PSNR | SSIM | MAE | PSNR | SSIM |
| IREDSWD [16] | Db1 | 13.163 | 26.215 | 0.659 | 21.561 | 26.971 | 0.515 |
| | Sym 2 | 12.834 | 27.770 | 0.718 | 19.198 | 27.022 | 0.577 |
| | Bior 1.3 | 14.012 | 27.117 | 0.692 | 19.115 | 27.106 | 0.433 |
| DWTSIRE [17] | Db1 | 13.524 | 27.521 | 0.688 | 19.521 | 27.312 | 0.543 |
| | Sym 2 | 11.530 | 27.510 | 0.761 | 16.988 | 27.739 | 0.626 |
| | Bior 1.3 | 13.442 | 27.130 | 0.682 | 20.617 | 27.265 | 0.539 |
| DASR [14] | Db1 | 16.371 | 27.305 | 0.685 | 19.841 | 27.442 | 0.540 |
| | Sym 2 | 15.858 | 27.176 | 0.758 | 18.167 | 27.578 | 0.626 |
| | Bior 1.3 | 17.113 | 27.125 | 0.676 | 20.707 | 27.313 | 0.532 |
| WDIRECS [15] | Db1 | 13.992 | 27.311 | 0.673 | 16.957 | 27.726 | 0.532 |
| | Sym 2 | 12.028 | 27.718 | 0.756 | 14.493 | 28.130 | 0.625 |
| | Bior 1.3 | 13.946 | 27.318 | 0.674 | 16.920 | 27.736 | 0.532 |
| Proposed sr technique | Db1 | 7.631 | 30.953 | 0.734 | 7.315 | 31.111 | 0.583 |
| | Sym 2 | **5.542** | **31.946** | **0.778** | **5.858** | **31.774** | **0.623** |
| | Bior 1.3 | 6.813 | 31.261 | 0.729 | 6.477 | 31.363 | 0.580 |

**Table 2** Objective criteria values of the resolution enhancement from 128x128 to 512x512. (The LR image is contaminated by Gaussian noise PSNR=17 dB)

| SR Methods | | Medical-1 | | | Medical-2 | | |
|---|---|---|---|---|---|---|---|
| | | MAE | PSNR | SSIM | MAE | PSNR | SSIM |
| IREDSWD [16] | Db1 | 14.929 | 18.918 | 0.786 | 9.821 | 20.415 | 0.906 |
| | Sym 2 | 10.921 | 22.350 | 0.819 | 8.536 | 22.621 | 0.915 |
| | Bior 1.3 | 14.269 | 19.600 | 0.747 | 11.806 | 19.959 | 0.889 |
| DWTSIRE [17] | Db1 | 11.138 | 21.841 | 0.804 | 10.192 | 22.181 | 0.915 |
| | Sym 2 | 9.959 | 22.412 | 0.828 | 8.379 | 23.259 | 0.930 |
| | Bior 1.3 | 11.753 | 20.212 | 0.797 | 9.500 | 22.178 | 0.916 |
| DASR [14] | Db1 | 11.154 | 21.786 | 0.807 | 10.180 | 22.175 | 0.916 |
| | Sym 2 | 10.217 | 23.399 | 0.824 | 8.793 | 22.977 | 0.929 |
| | Bior 1.3 | 11.395 | 21-628 | 0.792 | 10.213 | 22.090 | 0.915 |
| WDIRECS [15] | Db1 | 10.904 | 22.297 | 0.811 | 9.671 | 22.395 | 0.929 |
| | Sym 2 | 10.131 | 23.987 | 0.821 | 8.616 | 23.334 | 0.927 |
| | Bior 1.3 | 10.924 | 22.863 | 0.805 | 9.743 | 22.534 | 0.929 |
| PROPOSED SR TECHNIQUE | Db1 | 10.699 | 22.442 | 0.812 | 9.599 | 22.924 | 0.934 |
| | Sym 2 | **9.844** | **24.063** | **0.828** | **8.365** | **23.625** | **0.937** |
| | Bior 1.3 | 10.830 | 22.288 | 0.809 | 9.612 | 22.909 | 0.934 |

**Table 3** Objective criteria values of the resolution enhancement from 128x128 to 512x512. (The LR image is contaminated by Gaussian noise PSNR=17 dB

Numerous statistical simulations that we realized using databases that contain the test images of different nature (satellite, medical, optical, etc.) that are characterized by varying texture, details and edges, properties have confirmed the better performance of proposed method in resolution enhancement guaranteeing it robustness.

## Conclusions

In this work, a novel resolution-enhancement technique based on the interpolation of the HF sub-band images in the wavelet domain is presented. In contrast with other state-of-the-art resolution-enhancement techniques, the designed framework applies the edge and fine features information that is obtained from the HF sub-band images in wavelet transform space, NLM denoising algorithm modifying them for the SR restoration, and performs the sparse interpolation over an oriented block (approximations and details) in an LR image. All of these steps result in image resolution enhancement.

ISSN 2524-2121

Numerous simulation results on images from databases of different nature (satellite, medical, optical) have confirmed superiority of the proposed enhancement framework in performing the SR reconstruction while employing different wavelet function in comparison with other conventional methods. Experimental results have demonstrated better performance and robustness of the proposed algorithm in terms of objective criteria (PSNR, MAE and SSIM), as well as in the subjective perception via the human visual system.

**References**

Castillejos, H., Ponomaryov, V., Nino-de-Rivera, L. and Golikov, V., "Wavelet Transform Fuzzy Algorithms for Dermoscopic Image Segmentation," Computational and Mathematical Methods in Medicine, doi: 10.1155/2012/578721, (2012).

X. Li and M. T. Orchard (2001), ―New edge-directed interpolation‖. *IEEE Trans. Image Process*. vol. 10, No. 10, pp. 1521–1527. Kinebuchi, D. D. Muresan, and T. W. Parks (2001), ―Image interpolation using wavelet based hidden Markov trees‖, in *Proc. IEEE ICASSP*, vol. 3, pp. 7–11.

S. Zhao, H. Han, and S. Peng (2003), ―Wavelet domain HMT-based image super resolution‖, *Proc. IEEE ICIP*, Vol. 2, pp. 933–936.

A. Temizel and T. Vlachos (2005), ―Image resolution up-scaling in the wavelet domain using directional cycle spinning,‖ *J. Electron. Imaging*, Vol. 14, No. 4, p. 040501.

A. Gambardella and M. Migliaccio (2008), ―On the super-resolution of microwave scanning radiometer measurements‖, *IEEE. Trans. Geoscience and Remote Sensing* Letters, Vol. 5, No. 4, pp. 796–800.

M. Elad, M. A. T. Figueiredo, and Y. Ma. (2010) ―On the role of sparse and redundant representations in image processing‖. Proc. of IEEE, 98(6):972–982.

Chavez-Roman, H. and Ponomaryov. V., ―Super Resolution Image Generation Using Wavelet Domain Interpolation with Edge Extraction Via a Sparse Representation,‖ IEEE Geoscience and Remote Sensing Letters, doi: 10.1109/LGRS.2014.2308905, (2014).

H. Chavez, V. Gonzalez, A. Hernandez, and V. Ponomaryov ―Super Resolution Imaging via Sparse Interpolation in Wavelet Domain with Implementation in DSP and GPU‖, Lecture Notes in Computer Science, LNCS 8827, pp. 973–981, 2014.

M. Elad, J. L. Starck, P. Querre, and D. L. Donoho (2005), ―Simultaneous cartoon and texture image inpainting using morphological component analysis (MCA),‖ Appl. Comput. Harmon. Anal, vol. 19, pp. 340–358.

M. J. Fadili, J. L. Starck, and F. Murtagh (2007), ―Inpainting and zooming using sparse representations,‖ Comput. J.

V. Kravchenko, H. Meana, and V. Ponomaryov (2009), ―*Adaptive Digital Processing of Multidimensional Signals with Applications*‖, FizMatLit, Edit, Moscow, Russia, http://www.posgrados.esimecu.ipn.mx/.

E. Ramos, V. F. Kravchenko and V. Ponomaryov (2011), ―Efficient 2D to 3D video conversion implemented on DSP‖, *EURASIP Journal on Advances in Signal Processing*, doi:10.1186/1687.

G. Anbarjafari and H. Demirel (2010), ―Image Super Resolution Based on Interpolation of Wavelet Domain High Frequency Sub-bands and the Spatial Domain Input Image‖, *ETRI Journal*, vol. 32, No. 3, pp. 390-394.

Temizel A. and Vlachos T. (2005), ―Wavelet domain image resolution enhancement using cycle-spinning‖, Elect. Lett.,vol. 41, Issue 3, pp.:119 – 121.

H. Demirel and G. Anbarjafari (2011), ―Image Resolution Enhancement by Using Discrete and Stationary Wavelet Decomposition‖, *IEEE Trans. Image Processing*, Vol. 20, Is. 5, pp. 1458-1460.

H. Demirel and G. Anbarjafari (2011), ―Discrete Wavelet Transform-Based Satellite Image Resolution Enhancement‖, *IEEE Trans. Geoscience and Remote Sensing*, Vol. 49, Is. 6, pp. 1997-2004. http://peipa.essex.ac.uk/benchmark/databases/index.html

http://sipi.usc.edu/database/

M. Protter, M. Elad, H. Takeda, and P. Milanfar (2009), ―Generalizing the nonlocal-means to super-resolution reconstruction,‖ *IEEE Trans. Image Process.*, vol. 18, no. 1, pp. 36–51.

A. Buades, B. Coll, and J. M. Morel (2005), ―A review of image denoising algorithms, with a new one,‖ Multisc. Model. Simul., vol. 4, no. 2, pp. 490-530.

S. Mallat and G. Yu (2010), ―Super-Resolution with Sparse Mixing Estimators‖, IEEE Trans. on Image Process. Vol.19, Issue 11 pp.2889-2900. DOI: 10.1109/TIP.2010.2049927.

S. Mallat (2008), ―A Wavelet Tour of Signal Processing: The Sparse Way‖, 3rd ed. New York: Academic.

L. Feng, C. Y. Suen, Y.Y. Tang and L.H. Yang (2000), ―Edge Extraction of Images by Reconstruction Using Wavelet Decomposition Details at Different Resolution Levels‖, Int J. Patt. Recogn. Artif. Intell.,Vol.14, Issue 6, pp. 779-793. DOI: 10.1142/S0218001400000519.

Z. Wang, A. Bovik (2009), ―Mean Squared Error: Love It or Leave It? A new look at signal fidelity measures,‖ IEEE Signal Proc. Magazine, Vol.26, No.1, pp. 98-117.

Z.Wang, A. Bovik, H. Seikh and E. Simoncelli (2004), ―Image Quality Assessment: From Error Visibility to Structural Similarity‖. IEEE Trans. Image Process., vol. 13, No. 4, pp. 600-612

ISSN 2524-2121

**Article** **ECORFAN Journal- Taiwan**
June, 2020 Vol.4 No.7 28-34

# Prototype robot rover with Arduino, LabVIEW and mobile devices

# Prototipo de robot rover con Arduino, LabVIEW y dispositivos móviles

BELTRAN, Miguel†, SALINAS, Oscar and LUNA-ORTIZ, Martha

*Universidad Tecnológica Emiliano Zapata del Estado de Morelos. Universidad Tecnológica No. 1 C.P. 62760 Emiliano Zapata, Morelos*

ID 1st Author: *Miguel, Beltran*

ID 1st Coauthor: *Oscar, Salinas*

ID 2nd Coauthor: *Martha, Luna-Ortiz*

**DOI**: 10.35429/EJT.2020.7.4.28.34 Received March 22, 2020; Accepted June 11, 2020

**Abstract**

Terrestrial robot prototype all – terrain explorer, for exploration of areas that pose a danger to humans was developed. Mega Arduino microcontroller was used for remote control of the robot's movements as well as shipping and receiving signals in a wireless way. The visual interface is adapted to be used with mobile devices, with which the robot can be controlled, and also signal processing for decision- making. This visual interface was developed in LabVIEW executable mode, so this software not need be installed on the mobile device. A comparison between RF technologies and Wi - Fi point to point, no significant difference was found between them, with respect to the wireless functionality of the robot. The terrestrial prototype designed has four wheels, it is functional is independent and can be moved into different types of surface and places where humans cannot access, either for safety or for the same site. The proof of concept was successful, the prototype is expandable in functionality, appropriate technologies and application-specific functions can be integrated into the overall scheme.

**Autonomic Robot, Signal analysis, Arduino, Mobile Devices**

**Resumen**

Se desarrolló un prototipo de robot explorador terrestre tipo todo terreno, para exploración de áreas que representen un peligro para el ser humano. El microcontrolador Arduino Mega se utilizó para el control remoto de los movimientos del robot así como del envío y recepción de señales de manera inalámbrica. La interfaz visual se adapta para el uso con dispositivos móviles, con la cual se puede controlar el robot, así como el procesamiento de señales para la toma de decisiones. Esta interfaz visual fue desarrollada en LabVIEW en modo de archivo ejecutable, por lo que no es necesario tener instalado el software en el dispositivo. Se hizo una comparación en desempeño de tecnologías RF y Wi– Fi punto a punto, no se encontró diferencia significativa entre ellas, con respecto a la funcionalidad inalámbrica del robot. El prototipo diseñado terrestre tiene cuatro llantas, es funcional es autónomo y se puede desplazar en diferentes tipos de superficie, y lugares donde el ser humano no puede acceder, ya sea por seguridad o por la misma accesibilidad. La prueba de concepto se realizó con éxito, el prototipo es expandible en funcionalidad, se pueden integrar al esquema general tecnologías y funciones adecuadas para aplicaciones específicas.

**Robot autónomo, Análisis de señales, Arduino, Dispositivos Móviles**

**Citation:** BELTRAN, Miguel, SALINAS, Oscar and LUNA-ORTIZ, Martha. Prototype robot rover with Arduino, LabVIEW and mobile devices, ECORFAN Journal-Taiwan. 2020. 4-7: 28-34

† Researcher contributing as first author.

## Introduction

Historically humans have used machines to help with difficult tasks to perform, to make more efficient use of time or simply to provide comfort. These machines can be simple or very complicated, depending on the situation it faces, and the type of solution required. In the case of areas inaccessible to humans, either by the difficulty itself or because it represents a risk to humans, machines are useful to explore these areas. Therefore is possible to explore in a safer way areas that represent a danger to human access, and are to be considered at risk or be simply inaccessible.

There are two complicated situations for a human being can access a specific area: a disaster area and unexplored area. A disaster area most of the times implies a risk for humans to get in it. A disaster area is one where a particular natural phenomenom occured, a tornado, an earthquake for instance. It means an emergency situation needs to be attended, and some times the level of disaster do not let humans explore some small areas by themselves.

A disaster area in addition to the damage already done is an imminent risk to persons accessing this, either out of necessity or to help someone else. If one person is getting caught due to a natural disaster another important thing related with this issue is the rescuing time. Both are important survival factors, getting caugth is only a matter of fortune, the second depends on many factors, and is the difference between surviving or not. In an unexplored area there is also risk because people do not know what it will find in it, and thus it is almost impossible to estimate the risk for a human being to access. For both situations the common solution is to use some kind of tool to solve the problem without jeopardizing the life of someone else in rescuing people, or unforeseen risks in unexplored areas.

For instance, an autonomous robot which can access both areas of risk for human beings can be an adequated solution. The Robot must have autonomy to be able to explore area controlled remotely outside of the area. This must be done by a wireless control system, developed based on any wireless technology (IEEE Standard, 2012).

An image acquisition device is needed to get information about the general conditions of the area, and get an idea about the level of the risk, adquired images, either video or pictures, and data have to be transmitted by wireless connection. Temperature and humidity sensors, gas sensors, light sensors, to have an overview of the conditions of the environmental conditions of the area. Another important factor of auntonomy is that the robot must be able to avoid obstacles. It needs to detect them identify if is fixed or mobile and wait to it disappear or avoid it, respectively.

The researching idea came watching a video about the earthquake in 1985 at México City. Professors and students of Mechatronics Engineering review the documentary and ask themselves: What about if we build an explorer robot? It can do the risky work instead of called―human moles‖. After that the next objective was raise: Design and build a prototype robot type land rover to explore areas of risk, with sending and receiving signals by wireless telecommunication, and it can be controlled from a mobile device.

In literature are reported different types of rover, which have various forms and applications (Arévalo, 2014) (Ortíz, 2007) (Bauer, 2009) (Lidoris, 2009) (Acosta, 2013) (Villafuerte & Guzmán, 2014) (Oliva, 2011) (Rodrigo, 2014) (Bauer, 2009) (Sirish & Suresh, 2014). However the characteristics of this robot are no reported, for example the integration of Arduino and LabVIEW for a similar technological application is no reported so far.

The structure of this report is as following:

– Abstract.
– Introduction.
– Theoretical perspective.
– Hypothesis approach.
– Methodology.
– Results.
– Conclusions.
–

Students were involved in the project development, because for authors is important to involve students in the researching process and project managment to get autonomous behavior.

ISSN 2524-2121

**Theoretical perspective**

Today technology has had an unprecedented development in the history of mankind. After the steam era, followed the age of electricity, which is to say that was founded in 1808 with David Humpry (BBC, 2014). Almost a century after Nikola Tesla gave social life the way we know it today.

Thanks to Tesla have the generation and distribution of electricity current (conventional network) and wireless telecommunications. George Westinghouse commented laconically: without Tesla's contributions today's world would be impossible. (Steathskater, 2014) (Company, 2013) (Wordpress, 2012). These are the foundations of knowledge on which rests the breakthrough of current technology. Perform a technological development that would coordinate different technological areas to develop a work product that has the added value of social impact, is the motivation of the authors and students.

The equation could be as easy as: Technology (Electrical + Wireless telecommunication + mechanical + electronic) + social impact = Robot land rover explorer prototype. Telecommunications technology is used to send the information remotely and electronic technology is basically used to control the robot movements, processing data and convert them to information for making desitions. This taks are performed by a microcontroller. Microcontrollers are very dynamic electronic tools for building automation systems and elaborate and efficient control. The Arduino is a low cost open source microcontroller, which is easyto use and has diverse uses and applications (Arduino, Arduino, 2012), (Salinas, Low cost solarimetric station with solar resource calculation based on Arduino microcontroller and web platform, 2014), (Diana, 2015).

For wireless telecommunication there are two options: RF point to point and Wi – Fi one. Generally RF itself is taken as a synonymous of high-frequency signals and wireless telecommunication, describing anything from AM radio between 535 kHz and 1.605 MHz to computer local area networks (LANs) at 2.4 GHz. However, RF has traditionally defined frequencies from a few kHz to roughly 1 GHz. In some cases it is extended to 300 GHz to consider microwave frequencies as RF ones (Instruments, 2011). Arduino can work for wireless telecommunication either with Xbee (Arduino, Arduino, 2012) or Wi – Fi shield (Arduino, 2013). The first one allows Arduino microcontroller to communicate by Zigbee protocol, which is a standard for low power mesh networks working robustly. A comparison about the main technological characteristics about wireless connection is presented at Table

According to the data wireless telecommunication using Zigbee (XBee shield) should be the best option for land rover robot, Table 1, the only disadvantage is the low data rate, comparing to Wi – Fi, it means communication is going to be slow but cost, power consumption, complexity and coverture ratio must be better. ZigBee (Arduino Xbee shield) has been designed for applications that require safe communications with low data rate and low power consumption to maximize the usefull live of batteries, actually is more oriented to home automation systems (Diana, 2015) (Vázquez, Salinas, & Guillermo, Universidad Tecnológica Emiliano Zapata del Estado de Morelos, 2014) (Vázquez D. U., 2014) (Srinivasan, Raajan, Manonmani, & P, 2014) (Negus, Stephens, & Lansford, 2000). Arduino Xbee looks like the adequated one for the proposed robot, however one important point to keep in mind is about the image processing capability, due to one of the main purposes of the robot is get images from the unknown or disaster area.

| Technological parameter | Xbee | Wi - Fi |
|---|---|---|
| Coverture ratio (m) | Indoor: 305; Outdoor 914 | Indoor: (802.11b) 35 ; (802.11g) 38; Outdoor: 802.11b/g 140 |
| Date rate (Mb/s) | 0.020, 0.040 and 0.250 | From 2 to 11 aproximately |
| Power consumption | Low | Medium |
| Cost | Low | Medium |
| Complexity | Low | Medium |
| Frequency (GHz) | 2.4 | 2.4 |
| Security | Medium | WEP / WPA2 |

**Table 1** Comparison betweenZigbee and Wi – Fi, about characteristics for the proposed land rover robot (IEEE Standard, 2012)

Laboratory Virtual Instrumentation Engineering Workbench (LabVIEW) is an Integrated Development Environment oriented to virtual instrumentation. According with National Instruments definition: ―LabVIEW is a highly productive development environment for creating custom applications that interact with real-world data or signals in fields such as science and engineering‖ (National Instruments, 2013).

It is a very usefull electronic and programming tool, it is not a simple simulator, to test simple or complex integral electronic elements, such as controls, indicators, actuators, measurement instruments and so on. Engineers, scientists or students can convert their ideas to the reality in a not easy but neither very complex way, since programation is based in objects, not in code lines. Therefore is an adequated tool to develop systems to get and analize data to make decisions. LabVIEW is compatible with mobile devices, the visual interface can be designed and built with LabVIEW and save into device mobile as an exe file.

The exponential rise of mobile devices has caused more and more users prefer them instead of desktop computers. For example, to have the first 1000 million mobile subscribers passed 20 years, and only 15 months to get the other 1 billion. CISCO company predicted that this year 2015 will have the same number of mobile phones that human beings on the planet, and by 2020 there will be around 50 000 million of mobile devices users connected to the network, an average of three for each human being (Deloitte, 2013). Also there is the growth of the so-called App Economy, which is of 1 000 million smartphone users. This is an economy that generated 20 000 million of United States dolars (usd) at year 2011 (Deloitte, 2013). Therefore is very important to keep in mind this data, when every technological development, actually every kind of product, is going to be developed to be innovative and launch to the market.

## Hypothesis approach

Currently the technological advancement has allowed the technology is available to almost everyone. The cost of technology is becoming more accessible even for low budget universities.

This allows technologists researchers to design and build computers that have the same performance as those of trade, or the design of new and innovative technological applications brands. Therefore one hypothesis can be written:

Hypothesis: It is possible to build a working prototype rover autonomic, based on Arduino and LabVIEW, which allows sending signals and control remotely.

## Methodology

The methodology is simple, Figure 1, and is basically the one suggested by Sampieri (Sampieri, 2010). The researcing idea of technological development emerges as a local need for exploration unsafe for human being areas which may not or areas where disaster strikes explored. In the metropolitan area of the city of Cuernavaca Morelos, Mexico, due to a problem of over population, people have the need to locate their homes in unsafe areas, which are in constant danger of being in a disaster situation. Therefore the need to build an autonomous robot was raised for access to these areas in cases of a disaster, without putting in risk other human beings.

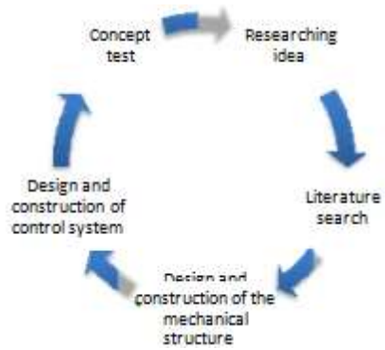


**Figure 1** Conceptual map of used methodology

Upon review of the literature no similar technological developments are found, which can occur that are integrating three types of teconlogías: mechanical, wireless communications and mobile devices. In addition to integration of Arduino programming in LabVIEW is recent (Instruments, 2011). The design of the mechanical structure is proper and craft, he drew on the expertise of automotive mechanical technicians.

This design is empirical, and everything is based on the experience of mechanical mechanical technician rather than an educated design and structural calculations. This is because no team member has expertise in mechanical structures.

The wireless electronic control system is developed based on Arduino and LabVIEW. Although elements for Arduino have been added to LabVIEW, programming the signal acquisition and processing them is not so trivial. As an added value presented in this prototype, it has functionality that can be controlled from a mobile device. This is accomplished by having the program in LabVIEW executable, so you should not have installed the software on the mobile device. Following this procedure the prototype was designed and developed.

## Results

The initial prototype is built aluminum profiles and acrylic material mechanical structure. The prototype has eight standard type tires, which have their own strength, to have the facility to move in any terrain. The tires at upper are to have a smooth ride and give strength to the robot to climb on land with steep slopes.

The robot has an automated mechanical arm that allows low weight lifting and moving objects. This arm is commercial, it was not built by the authors, just programmed, Figure 2. The utility of the arm is still under study because at this stage, priority is the prototype autonomous mobility. LabVIEW programming environment is graphic, designed for virtual instrumentation. This allows a versatile and dynamic programming, where you can simulate the behavior of components without having physically connected.

**Figure 2** Autonomous explorer robot prototype

It also allows physical interaction with measuring instruments and sensors on one card automatic data acquisition. The whole program is not possible to show in a figure, so that in Figure 3 is showed a screenshot of part of it.

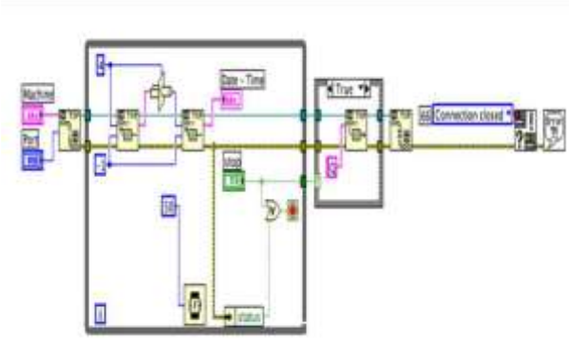

**Figure 3** Part of the virtual programation in LabVIEW

LabVIEW allows custom user interfaces, which are suitable for mobile devices, Figure 4. The interface shown in Figure 4 is the one where the user can control the features of land rover explorer robot. With this interface user are able to control: the movement of the robot using touch button; sending signals to the robot; acquiring signals from the robot and processing the basic data for decision-making. You can turn the robot motion control using the accelerometer of electronic tablet, however at this stage is not covered.

**Figure 4** Visual interface for mobile devices

## Conclusions

It is possible to build a robot explorer combining functional autonomic free hardware (Arduino) and licensed control software (LabVIEW). Using Arduino microcontroller greatly reduces the cost of building the robot and does not impact the performance of the same, as it has the same functionality as other commercial microcontroller.

ISSN 2524-2121

Involving young students in developing technological developments have both academic research and business impact. Young people develop skills for autonomy since they themselves carry out basic research to implement a technological development.

They also recognize the on-going importance of teamwork and integration of multidisciplinary teams, as the skills of each other come together.

The proof of concept has been successful, and is able to keep improving the rover, working on their autonomy and also in the number of signals that can send and receive, to convert them into information to improve the decision making process.

**Acknowledgement**

The authors wish to thank to the students Martín Omar Vázquez Reyes, Luis David Aviles Wenceslao, Ángel Carlos Giles Jiménez y Gilberto Hernández Tumalán for their commitment in developing the prototype. For their dedication and professional work as well as all the ideas that have contributed to the design and optimal operation of the rover.

**References**

Acosta, L. (Abril de 2013). *Diseño y construcción de un robot explorador de terreno.* Obtenido de Universidad Salesiana: http://dspace.ups.edu.ec/handle/123456789/4498

Adán, E., Luna, M., Damián, E., Estrada, Á., & Salinas, O. (2014). Recorrido virtual interactivo de las instalaciones de la Universidad Tecnológica Emiliano Zapata del Estado de Morelos - UTEZ. *Ciencias de la Ingeniería y la Tecnología; Hnadbook T - V; ISSN 2007-1582, e-ISSN 2007-3862*, 272- 283.

Android. (2010). Recuperado el 20 de febrero de 2010, de https://www.android.com/

Arduino. (2000). *Arduino*. Recuperado el 10 de Abril de 2015, de Arduino: www.arduino.cc

Arduino. (12 de Octubre de 2013). *Arduino* Septiembre 2015 Vol.2 No.4 679-687 *WiFi Shield*. Recuperado el 12 de December de 2014, de http://www.arduino.cc/en/Main/ArduinoWiFiShield

Arduino. (14 de Ocutbre de 2013). *Arduino Xbee Shield*. Recuperado el 12 de December de 2014, de http://www.arduino.cc/en/pmwiki.php?n=Main/ArduinoXbeeShield

Arévalo, M. (01 de Mayo de 2014). *Escuela Politécnica Nacional, Ecuador.* Recuperado el 06 de Mayo de 2014, de http://ciecfie.epn.edu.ec/PROYECTOS/pdfs/Explorador1.pdf

Bauer, A. (april de 2009). The Autonomous City Explorer: Towards Natural Human-Robot Interaction in Urban Environments. *International Journal of Social Robotics , 1*(2), 127-140.

BBC. (25 de Abril de 2014). *BBC* . Recuperado el 25 de Abril de 2014, de BBC History Historic Figures: http://www.bbc.co.uk/history/historic_figures/davy_humphrey.shtml

Company, N. T. (20 de Enero de 2013). *Tesla Universe*. Recuperado el 20 de Enero de 2013, de Tesla Universe: http://www.teslauniverse.com/nikola-tesla-books

Deloitte. (2013). *Deloitte*. Recuperado el 12 de mayo de 2013, de http://www2.deloitte.com/content/dam/Deloitte/co/Documents/technology-media-telecommunications/TMTPredictions/Deloitte%20Predicciones%20TMT%202013.pdf

Diana, V. (2015). Control de Luces vía Wi-Fi con Arduino y Android. *UneTEZ*. EdneyWilliam A., A. (2003). *Real 802.11 Security: Wi-Fi Protected Access and 802.11i*. Boston, MA, USA: Addison-Wesley Longman Publishing Co., Inc. .

IEEE Standard. (2012). *IEEE Standard for information technology; Std 802.11(TM)- 2012.* New York: IEEE.

Instruments, N. (2011). *The LabVIEW Arduino Community has moved to LabVIEW MakerHub*. Recuperado el Ocubre de 2013, de https://decibel.ni.com/content/groups/labview-interface-for-arduino

Lidoris, G. (2009). The Autonomous City Explorer (ACE) project — mobile robot navigation in highly populated urban environments. *Robotics and Automation, 2009. ICRA '09. IEEE International Conference on* (págs. 1416-1422). IEEE.

National Instruments. (16 de August de 2013). *What is LabVIEW?* Recuperado el 6 de January de 2014, de http://www.ni.com/newsletter/51141/en/

National Instruments. (09 de December de 2014). *Introduction to RF & Wireless Communications Systems.* Recuperado el 15 de December de 2014, de http://www.ni.com/tutorial/3541/en/

Negus, K., Stephens, A., & Lansford, J. (2000). HomerRF: Wireless Networking for the Connected Home. *IEEE Personal Communications*, 20-27.

Oliva, J. (2011). *Diseño e implementación de robot explorador semiautónomo con celdas solares y tracción con orugas.* Concepción, Chile: Universidad de Concepción.

Ortíz, S. (2007). Robot móvil todo terreno. *6to.*

*Congreso Nacional de Mecatrónica* (págs. 8-10). Asociación de Mecatrónica A.C.

Rodrigo, C. (2014). *Estudio, Diseño e Implementación de un Prototipo de Robot Explorador y Enrutador de Cable.* Quito, Ecuador: Universidad Tencnológica de Israel, Tesis de Ingeniería.

Salinas, O. (Enero de 2014). Low cost solarimetric station with solar resource calculation based on Arduino microcontroller and web platform. *Energy and Environment focus, 2*, 1,5.

Sampieri, R. (2010). Metodología de la Investigación. (M. G. Hill, Ed.) México,

México: Mc Graw Hill.

Sirish, T., & Suresh, B. (2014). Rootic Control with Android & PC Using X-Bee. *International Journal of Applied Engineering Research*, 4639-4644.

Srinivasan, D., Raajan, N., Manonmani, & P. (2014). Intelligent Lighting Control Using Android Application. *International Journal of Applied Engineering Research*, 3361-3366.

Standards, I. (2005). *IEEE Std. 802.15.4 Enabling Pervasive Wireless Sensor Networks.* New York: IEEE Standars Association.

Tesla, N. (1900). *Patente nº 649576.* United States.

Vázquez, D. U. (16 de Octubre de 2014). Recuperado el Octubre16 de 2014, de https://www.youtube.com/watch?v=_PwlAx8S gYw

Vázquez, D., & UTEZ. (Octubre de 2015).

Vázquez, D., Salinas, O., & Guillermo, G. (16 de octubre de 2014). *Universidad Tecnológica Emiliano Zapata del. Estado de Morelos*. Recuperado el 12 de enero de 2015, de www.utez.edu.mx:https://www.youtube.com/watch?v=_PwlAx8S gYw

Vázquez, D., Salinas, O., & Wences, F. (2015). Control de luces vía Wi - Fi con Arduino y Android. *UneTEZ*, Enviado para publicar.

Villafuerte, M., & Guzmán, O. (2014). *Proceso de diesño de Rover para minería lunar. "NASA Lunabotics mining competition".* (T. d. UNAM, Ed.) México: UNAM.

Wordpress. (27 de 11 de 2012). *ENJTJournal*. Recuperado el 2 de Febrero de 2013, de Wordpresss: https://entjournal.wordpress.com/2012/11/27/nikola-tesla-and-his-discovery-of-wireless-technology/

# [Title in Times New Roman and Bold No. 14 in English and Spanish]

Surname (IN UPPERCASE), Name 1st Author†*, Surname (IN UPPERCASE), Name 1st Coauthor, Surname (IN UPPERCASE), Name 2nd Coauthor and Surname (IN UPPERCASE), Name 3rd Coauthor

*Institutional Affiliation of Author including Dependency (No.10 Times New Roman and Italic)*

*International Identification of Science - Technology and Innovation*

ID 1st Author: (ORC ID - Researcher ID Thomson, arXiv Author ID - PubMed Author ID - Open ID) and CVU 1st author: (Scholar-PNPC or SNI-CONACYT) (No.10 Times New Roman)

ID 1st Coauthor: (ORC ID - Researcher ID Thomson, arXiv Author ID - PubMed Author ID - Open ID) and CVU 1st coauthor: (Scholar or SNI) (No.10 Times New Roman)

ID 2nd Coauthor: (ORC ID - Researcher ID Thomson, arXiv Author ID - PubMed Author ID - Open ID) and CVU 2nd coauthor: (Scholar or SNI) (No.10 Times New Roman)

ID 3rd Coauthor: (ORC ID - Researcher ID Thomson, arXiv Author ID - PubMed Author ID - Open ID) and CVU 3rd coauthor: (Scholar or SNI) (No.10 Times New Roman)

(Report Submission Date: Month, Day, and Year); Accepted (Insert date of Acceptance: Use Only ECORFAN)

**Abstract (In English, 150-200 words)**

Objectives
Methodology
Contribution

**Abstract (In Spanish, 150-200 words)**

Objectives
Methodology
Contribution

**Keywords (In English)**

Indicate 3 keywords in Times New Roman and Bold No. 10

**Keywords (In Spanish)**

Indicate 3 keywords in Times New Roman and Bold No. 10

**Citation:** Surname (IN UPPERCASE), Name 1st Author, Surname (IN UPPERCASE), Name 1st Coauthor, Surname (IN UPPERCASE), Name 2nd Coauthor and Surname (IN UPPERCASE), Name 3rd Coauthor. Paper Title. ECORFAN Journal-Taiwan. Year 1-1: 1-11 [Times New Roman No.10]

* Correspondence to Author (example@example.org)
† Researcher contributing as first author.

## Introduction

Text in Times New Roman No.12, single space.

General explanation of the subject and explain why it is important.

What is your added value with respect to other techniques?

Clearly focus each of its features

Clearly explain the problem to be solved and the central hypothesis.

Explanation of sections Article.

## Development of headings and subheadings of the article with subsequent numbers

[Title No.12 in Times New Roman, single spaced and bold]

Products in development No.12 Times New Roman, single spaced.

## Including graphs, figures and tables-Editable

In the article content any graphic, table and figure should be editable formats that can change size, type and number of letter, for the purposes of edition, these must be high quality, not pixelated and should be noticeable even reducing image scale.

[Indicating the title at the bottom with No.10 and Times New Roman Bold]

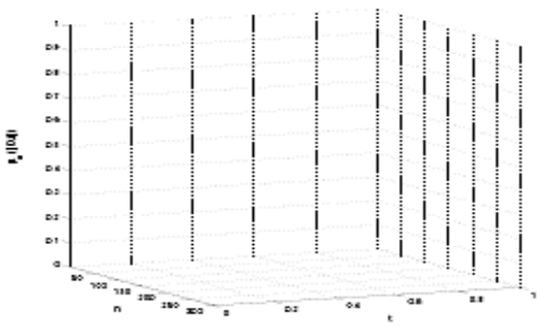

**Graphic 1** Title and *Source (in italics)*

Should not be images-everything must be editable.

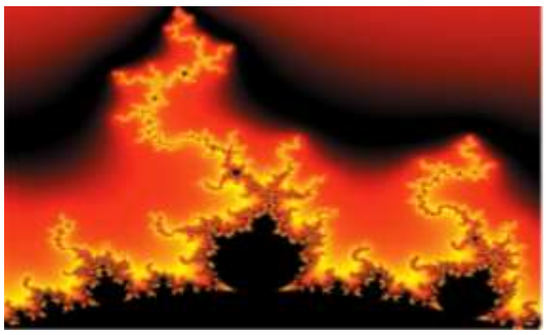

**Figure 1** Title and *Source (in italics)*

Should not be images-everything must be editable.

| | | | | |
|---|---|---|---|---|
| | | | | |
| | | | | |
| | | | | |
| | | | | |

**Table 1** Title and *Source (in italics)*

Should not be images-everything must be editable.

Each article shall present separately in **3 folders**: a) Figures, b) Charts and c) Tables in .JPG format, indicating the number and sequential Bold Title.

## For the use of equations, noted as follows:

$$Y_{ij} = \alpha + \sum_{h=1}^{r} \beta_h X_{hij} + u_j + e_{ij} \qquad (1)$$

Must be editable and number aligned on the right side.

## Methodology

Develop give the meaning of the variables in linear writing and important is the comparison of the used criteria.

## Results

The results shall be by section of the article.

## Annexes

Tables and adequate sources

## Thanks

Indicate if they were financed by any institution, University or company.

## Conclusions

Explain clearly the results and possibilities of improvement.

ISSN 2524-2121

**References**

Use APA system. Should not be numbered, nor with bullets, however if necessary numbering will be because reference or mention is made somewhere in the Article.

Use Roman Alphabet, all references you have used must be in the Roman Alphabet, even if you have quoted an Article, book in any of the official languages of the United Nations (English, French, German, Chinese, Russian, Portuguese, Italian, Spanish, Arabic), you must write the reference in Roman script and not in any of the official languages.

**Technical Specifications**

Each article must submit your dates into a Word document (.docx):

Journal Name
Article title
Abstract
Keywords
Article sections, for example:

*1. Introduction*
*2. Description of the method*
*3. Analysis from the regression demand curve*
*4. Results*
*5. Thanks*
*6. Conclusions*
*7. References*

Author Name (s)
Email Correspondence to Author
References

**Intellectual Property Requirements for editing:**

-Authentic Signature in Color of Originality Format Author and Coauthors

-Authentic Signature in Color of the Acceptance Format of Author and Coauthors

ISSN 2524-2121

**Reservation to Editorial Policy**

ECORFAN Journal-Taiwan reserves the right to make editorial changes required to adapt the Articles to the Editorial Policy of the Journal. Once the Article is accepted in its final version, the Journal will send the author the proofs for review. ECORFAN® will only accept the correction of errata and errors or omissions arising from the editing process of the Journal, reserving in full the copyrights and content dissemination. No deletions, substitutions or additions that alter the formation of the Article will be accepted.

**Code of Ethics - Good Practices and Declaration of Solution to Editorial Conflicts**

**Declaration of Originality and unpublished character of the Article, of Authors, on the obtaining of data and interpretation of results, Acknowledgments, Conflict of interests, Assignment of rights and Distribution**.

The ECORFAN-Mexico, S.C Management claims to Authors of Articles that its content must be original, unpublished and of Scientific, Technological and Innovation content to be submitted for evaluation.

The Authors signing the Article must be the same that have contributed to its conception, realization and development, as well as obtaining the data, interpreting the results, drafting and reviewing it. The Corresponding Author of the proposed Article will request the form that follows.

Article title:

– The sending of an Article to ECORFAN Journal- Taiwan emanates the commitment of the author not to submit it simultaneously to the consideration of other series publications for it must complement the Format of Originality for its Article, unless it is rejected by the Arbitration Committee, it may be withdrawn.

– None of the data presented in this article has been plagiarized or invented. The original data are clearly distinguished from those already published. And it is known of the test in PLAGSCAN if a level of plagiarism is detected Positive will not proceed to arbitrate.

– References are cited on which the information contained in the Article is based, as well as theories and data from other previously published Articles.

– The authors sign the Format of Authorization for their Article to be disseminated by means that ECORFAN-Mexico, S.C. In its Holding Taiwan considers pertinent for disclosure and diffusion of its Article its Rights of Work.

– Consent has been obtained from those who have contributed unpublished data obtained through verbal or written communication, and such communication and Authorship are adequately identified.

– The Author and Co-Authors who sign this work have participated in its planning, design and execution, as well as in the interpretation of the results. They also critically reviewed the paper, approved its final version and agreed with its publication.

– No signature responsible for the work has been omitted and the criteria of Scientific Authorization are satisfied.

– The results of this Article have been interpreted objectively. Any results contrary to the point of view of those who sign are exposed and discussed in the Article.

**Copyright and Access**

The publication of this Article supposes the transfer of the copyright to ECORFAN-Mexico, SC in its Holding Taiwan for its ECORFAN Journal- Taiwan, which reserves the right to distribute on the Web the published version of the Article and the making available of the Article in This format supposes for its Authors the fulfilment of what is established in the Law of Science and Technology of the United Mexican States, regarding the obligation to allow access to the results of Scientific Research.

Article Title:

| Name and Surnames of the Contact Author and the Coauthors | Signature |
|---|---|
| 1. | |
| 2. | |
| 3. | |
| 4. | |

**Principles of Ethics and Declaration of Solution to Editorial Conflicts**

**Editor Responsibilities**

The Publisher undertakes to guarantee the confidentiality of the evaluation process, it may not disclose to the Arbitrators the identity of the Authors, nor may it reveal the identity of the Arbitrators at any time.

The Editor assumes the responsibility to properly inform the Author of the stage of the editorial process in which the text is sent, as well as the resolutions of Double-Blind Review.
The Editor should evaluate manuscripts and their intellectual content without distinction of race, gender, sexual orientation, religious beliefs, ethnicity, nationality, or the political philosophy of the Authors.

The Editor and his editing team of ECORFAN® Holdings will not disclose any information about Articles submitted to anyone other than the corresponding Author.

The Editor should make fair and impartial decisions and ensure a fair Double-Blind Review.

**Responsibilities of the Editorial Board**

The description of the peer review processes is made known by the Editorial Board in order that the Authors know what the evaluation criteria are and will always be willing to justify any controversy in the evaluation process. In case of Plagiarism Detection to the Article the Committee notifies the Authors for Violation to the Right of Scientific, Technological and Innovation Authorization.

**Responsibilities of the Arbitration Committee**

The Arbitrators undertake to notify about any unethical conduct by the Authors and to indicate all the information that may be reason to reject the publication of the Articles. In addition, they must undertake to keep confidential information related to the Articles they evaluate.

Any manuscript received for your arbitration must be treated as confidential, should not be displayed or discussed with other experts, except with the permission of the Editor.

The Arbitrators must be conducted objectively, any personal criticism of the Author is inappropriate.

The Arbitrators must express their points of view with clarity and with valid arguments that contribute to the Scientific, Technological and Innovation of the Author.

The Arbitrators should not evaluate manuscripts in which they have conflicts of interest and have been notified to the Editor before submitting the Article for Double-Blind Review.

**Responsibilities of the Authors**

Authors must guarantee that their articles are the product of their original work and that the data has been obtained ethically.

Authors must ensure that they have not been previously published or that they are not considered in another serial publication.

Authors must strictly follow the rules for the publication of Defined Articles by the Editorial Board.

The authors have requested that the text in all its forms be an unethical editorial behavior and is unacceptable, consequently, any manuscript that incurs in plagiarism is eliminated and not considered for publication.

Authors should cite publications that have been influential in the nature of the Article submitted to arbitration.

**Information services**

**Indexation - Bases and Repositories**

RESEARCH GATE (Germany)
GOOGLE SCHOLAR (Citation indices-Google)
MENDELEY (Bibliographic References Manager)
HISPANA (Information and Bibliographic Orientation-Spain)

**Publishing Services**

Citation and Index Identification H
Management of Originality Format and Authorization
Testing Article with PLAGSCAN
Article Evaluation
Certificate of Double-Blind Review
Article Edition
Web layout
Indexing and Repository
ArticleTranslation
Article Publication
Certificate of Article
Service Billing

**Editorial Policy and Management**

69 Street. YongHe district, ZhongXin. Taipei-Taiwan. Phones: +52 1 55 6159 2296, +52 1 55 1260 0355, +52 1 55 6034 9181; Email: contact@ecorfan.org www.ecorfan.org

# ECORFAN Journal-Taiwan

"Solar Concentrator PDR with solar tracking"
**DURAN, Pino, BARBOSA, J. Gabriel, QUINTO, Pedro and MORENO, Luis**

"Mechatronic system to assist rehabilitation therapies for shoulder and elbow joints: Design, kinematic analysis, building and HMI"
**AGUILAR-PEREYRA, Felipe, ALVARADO, Jorge, ALEGRIA, Jesús and SOSA, José**
*Universidad Tecnológica de Querétaro*

"Image resolution enhancement via sparse interpolation on wavelet domain"
**CHAVEZ, Román, PONOMARYOW, Volodymyr and CASTRO, Fernando**
*Universidad Tecnológica de la Región Norte de Guerrero*

"Prototype robot rover with Arduino, LabVIEW and mobile devices"
**BELTRAN, Miguel, SALINAS, Oscar and LUNA-ORTIZ, Martha**
*Universidad Tecnológica Emiliano Zapata del Estado de Morelos*

2524 2121
ISSN 2524-2121

www.ecorfan.org